THE ASTROPHYSICAL JOURNAL, 197:85–115, 1975 April 1


# INTERSTELLAR ABSORPTION LINES IN THE SPECTRUM OF ZETA OPHIUCHI

DONALD C. MORTON
Princeton University Observatory
*Received 1974 August 12*

## ABSTRACT

Extensive high-resolution scans with the ultraviolet spectrometer on the *Copernicus* satellite have been combined with the available ground-based data on interstellar lines to obtain temperatures, densities, and abundances in H I clouds and H II regions in the direction of ζ Oph. Column densities have been obtained for 21 elements in various stages of ionization. A new determination for CO and the results for $H_2$, HD, CH, $CH^+$, and CN for other authors also have been included. In addition, upper limits have been reported for five elements and 11 molecules. In the ultraviolet scans, 45 lines remain unidentified. Radial velocities and curves of growth were used to locate the species seen in the ultraviolet into one or more of the six clouds already known from the visible spectra. The $H_2$, HD, and most of the neutral atoms are concentrated in one cloud at a heliocentric velocity of $-14.4$ km s$^{-1}$, while N I, O I, Ar I, and most of the first ions are distributed over at least two of these clouds. The velocities of the higher ion states implied there are H II regions in addition to the Strömgren sphere.

Calculations of the ionization equilibrium for C, Mg, S, and Ca have shown that the electron density $n_e \sim 0.7$ cm$^{-3}$ in the $-14.4$ km s$^{-1}$ cloud. Since the ionization of carbon is the primary source of the electrons, the ratio C II/H requires that $n_H \sim 10^4$ cm$^{-3}$ for the total hydrogen nuclei, with a fractional ionization $n_e/n_H \sim 7 \times 10^{-5}$. Both densities could be up to 20 times larger if the cloud is close to the star. The cloud must be no more than 0.05 pc thick. The populations of the fine-structure levels in the C I ground state require $T = 19°$ K. The HD and the excited rotational levels of $H_2$ need temperatures between 56° and 115°, though the lines appear to have the same velocity as the C I, probably indicating that the dense cloud must have some associated hotter regions.

Relative to hydrogen, most of the elements in the H I clouds are depleted by factors of 3 to 4000 compared with the solar system abundances. Only sulfur and zinc are present in the gas with near normal abundances. Several elements, particularly Al, Si, and Fe, appear to be depleted in the H II regions as well, but nitrogen is normal.

*Subject headings:* interstellar matter — spectra, ultraviolet

## I. INTRODUCTION

The visual spectrum of the bright O9.5 V star ζ Ophiuchi is well known for its many interstellar absorption lines. These lines have been selected for detailed studies by several authors including Herbig (1968), Hobbs (1973*a*), and Shulman, Bortolot, and Thaddeus (1974). In addition, rocket observations of the far-ultraviolet interstellar lines have been discussed by Smith and Stecher (1971), Smith (1972), and Jenkins (1973). A particular advantage for both visible and ultraviolet studies is the high stellar rotational velocity of $v \sin i = 396$ km s$^{-1}$ (Uesugi and Fukuda 1970), which permits an easy separation of the narrow interstellar lines from the broad stellar features. Consequently ζ Oph was the first star on the survey program of far-ultraviolet interstellar lines with the *Copernicus* satellite (Rogerson, Spitzer *et al.* 1973) and 7 months later it was the first star chosen for a complete scan at 0.05 Å resolution from 980 to 1420 Å. This paper combines the earlier *Copernicus* results, already reported by Morton *et al.* (1973), with a variety of later measurements to determine the interstellar column densities and abundance ratios of a large number of ion species which are detectable only above the Earth's atmosphere. The available visual data are included in the discussion to give a complete picture of the depletion of the heavy elements and the excitation and ionization conditions in the interstellar gas in the direction of ζ Oph.

Some selected results from the extensive *Copernicus* scans already have been reported in recent papers. Spitzer and Cochran (1973) and Spitzer, Cochran, and Hirshfeld (1974) have discussed the $H_2$ and HD lines; Morton, Smith, and Stecher (1974) have found an interesting upper limit on B II; de Boer *et al.* (1974) have analyzed the lines of Mn II and Fe II; and de Boer and Morton (1975) have studied the C I lines, including the populations of the fine-structure levels. In addition, Morton (1974) has used the column densities derived in the present paper to obtain interstellar element abundances relative to hydrogen in the clouds toward ζ Oph.

## II. OBSERVATIONS

### *a) Far-Ultraviolet Lines*

The *Copernicus* data presented in this paper were obtained with the two high-resolution detectors during the following four periods: 1972 August 28 to September 4, repeated scans of selected lines; 1973 April 4 to April 27, continuous scan from 980 to 1420 Å plus repeated scans of selected lines; 1973 August 27 and 28, repeated scans to search for B II λ1362.461; 1974 April 13 and 14, repeated scans of selected lines.

TABLE 1

INTERSTELLAR ATOMIC ULTRAVIOLET ABSORPTION LINES IN ζ OPHIUCHI

| Ion | $\lambda_{Lab}$ (Å) | Mlt. No. | $f$ | $\lambda_{Obs} - \lambda_{Lab}$ (Å) | $W_\lambda$ (mÅ) | m.e. (mÅ) | No. Obs. | Remarks |
|---|---|---|---|---|---|---|---|---|
| H I..... | 1215.670 | 1 | 0.4162 | ... | 16700 | 300 | 1 | 2 lines |
| | 1025.722 | 2 | 0.0791 | ... | ... | | 1 | blend with $H_2$(6,0) |
| B II..... | 1362.461 | 1 | 0.827 | ... | < 1.3 | | 25 | |
| C I..... | 1328.833 | 4 | 0.12† | −0.018 | 52 | 6 | 5 | |
| | 1280.135 | 5 | 0.028† | −0.015 | 34 | 2 | 3 | |
| | 1277.245 | 7 | 0.16† | ... | 74 | | 1 | including C I* 7 |
| | 1276.482 | 7.01 | 0.012† | −0.004 | 24.9 | | 1 | |
| | 1270.143 | 8.01 | ... | +0.004 | 10.6 | | 1 | |
| | 1260.736 | 9 | 0.038 | −0.016 | 38 | | 1 | |
| | 1193.996 | 9.02 | 0.0094† | −0.021 | 18.6 | | 1 | blend with C I** 9.02 |
| | 1193.031 | 11 | 0.05† | −0.021 | 54 | 2 | 3 | blend with C I* 11 |
| | 1192.218 | 12 | 0.003† | −0.014 | 15.3 | | 1 | |
| | 1190.021 | 13.01 | ... | −0.005 | 11.1 | 3.0 | 5 | |
| | 1188.833 | 14 | 0.017† | −0.017 | 25.3 | | 1 | blend with Cl I |
| | 1158.324 | 15.01 | 0.003† | −0.013 | 16.1 | | 1 | |
| | 1157.910 | 16 | 0.03† | −0.011 | 30 | | 1 | |
| | 1157.186 | 17 | 0.0005† | −0.002 | 7.9 | | 1 | |
| | 1155.809 | 19 | 0.02† | −0.007 | 21.5 | | 1 | |
| | 1140.010 | 21.01 | ... | −0.008 | 14.3 | 3.0 | 2 | blend with C I* 22 |
| | 1139.789 | 22 | ... | −0.004 | 42 | | 1 | blend with C I* 21.01 |
| | 1138.383 | 23 | 0.004† | −0.010 | 16.8 | | 1 | |
| | 1129.318 | 24.01 | ... | −0.005 | 14.4 | | 1 | blend with C I* 25 |
| | 1129.196 | 25 | ... | −0.029 | 31 | | 1 | including C I*, C I** 25 |
| | 1128.477 | 25.01 | 0.0003† | −0.007 | 9.2 | | 1 | |
| | 1128.075 | 26 | ... | −0.013 | 7.9 | | 1 | |
| | 1128.171 | 26.01 | 0.0011† | −0.010 | 9.1 | | 1 | |
| | 1122.518 | 26.03 | 0.0004† | ... | ... | | | blend with Fe III |
| | 1122.447 | 27 | 0.007† | −0.017 | 16.2 | 3.3 | 2 | |
| | 1121.713 | 27.01 | ... | −0.003 | 10.0 | | 1 | blend with C I* 27.03 |
| | 1121.520 | 27.03 | ... | −0.018 | 11.4 | | 1 | unidentified blend |
| C I*..... | 1560.70 | 3 | 0.081 | +0.05 | 50: | | 4 | 2 lines |
| | 1329.101 | 4 | 0.12† | −0.017 | 60 | 5 | 3 | 3 lines |
| | 1280.597 | 5 | 0.0092† | −0.020 | 20.4 | | 1 | |
| | 1280.404 | 5 | 0.0070† | −0.017 | 15.6 | | 1 | blend with C I** 5 |
| | 1279.890 | 5 | 0.012† | −0.015 | 18.5 | 1.0 | 3 | |
| | 1279.056 | 6 | 0.0016† | −0.010 | 10.8 | | 1 | |
| | 1277.513 | 7 | 0.04† | ... | 39 | | 1 | including C I** 7 |
| | 1276.750 | 7.01 | 0.0016† | −0.005 | 10.6 | | 1 | |
| | 1261.122 | 9 | 0.016 | −0.013 | 15.2 | 2.1 | 2 | |
| | 1260.996 | 9 | 0.0095 | −0.008 | 18.6 | | 1 | blend |
| | 1260.927 | 9 | 0.013 | −0.015 | 22.4 | | 1 | blend |
| | 1194.406 | 9.02 | 0.0031† | −0.009 | 11.9 | | 1 | |
| | 1194.229 | 9.02 | 0.0024† | −0.012 | 7.9 | | 1 | blend with C I* 10 |
| | 1193.679 | 9.02 | 0.0039† | −0.015 | 15.8 | | 1 | blend with C I** 11 |
| | 1194.301 | 10 | ... | −0.011 | 10.4 | | 1 | blend with C I* 9.02 |
| | 1192.451 | 12 | 0.002† | −0.004 | 12.5 | | 1 | |
| | 1189.249 | 14 | 0.0070† | −0.013 | 12.2 | | 1 | |
| | 1189.065 | 14 | 0.0042† | −0.018 | 16.3 | | 1 | blend |
| | 1188.992 | 14 | 0.0056† | −0.002 | 12.7 | | 1 | blend |
| | 1158.544 | 15.01 | 0.0009† | 0 | 5.7 | | 1 | |
| | 1158.035 | 15.01 | 0.0014† | −0.015 | 23.4 | | 1 | including C I** 16 |
| | 1158.130 | 16 | 0.007† | −0.009 | 11.0 | | 1 | including C I** 16 |
| | 1157.770 | 16 | 0.02† | −0.004 | 12.6 | | 1 | including C I** 17 |
| | 1157.405 | 17 | 0.0009† | +0.019 | 7.3 | | 1 | identity uncertain |
| | 1156.00 | 19 | 0.013† | 0 | 37 | | 1 | 2 lines |
| | 1139.514 | 22 | ... | 0 | 6.7 | | 1 | |
| | 1139.300 | 22.01 | ... | +0.002 | 5.4 | | 1 | |
| | 1138.595 | 23 | 0.0011† | −0.025 | 19.4 | | 1 | blend with C I 22.03 |
| | 1129.749 | 25 | ... | +0.001 | 3.4 | | 1 | |
| | 1129.078 | 24.01 | ... | −0.010 | 16.0 | | 1 | identity uncertain |
| | 1128.686 | 25.01 | 0.003† | −0.012 | 9.9 | | 1 | |
| | 1128.27 | 26 | ... | −0.01 | 10.7 | | 1 | 2 lines |
| | 1122.75 | 26.03 | 0.0003† | +0.01 | 10.1 | | 1 | 2 lines + C I* to 3F° |
| C I**..... | 1561.42 | 3 | 0.013 | −0.02 | 50: | | 4 | 2 lines |
| | 1329.584 | 4 | 0.12† | −0.012 | 33 | | 1 | 2 lines |
| | 1280.847 | 5 | 0.0070† | −0.012 | 9.9 | | 1 | |
| | 1280.333 | 5 | 0.021† | −0.011 | 12.2 | | 1 | blend with C I* 5 |
| | 1279.498 | 6 | 0.001† | −0.035 | 3.7 | | 1 | uncertain feature |
| | 1279.229 | 6 | 0.004† | −0.004 | 9.3 | | 1 | |
| | 1277.954 | 7 | 0.0016† | −0.014 | 2.4 | | 1 | |

TABLE 1—*Continued*

| Ion | $\lambda_{Lab}$ (Å) | Mlt. No. | $f$ | $\lambda_{Obs} - \lambda_{Lab}$ (Å) | $W_\lambda$ (mÅ) | m.e. (mÅ) | No. Obs. | Remarks |
|---|---|---|---|---|---|---|---|---|
| C I** *contd.*... | 1277.723 | 7 | 0.02† | −0.008 | 13.8 | | 1 | |
| | 1261.552 | 9 | 0.028 | −0.004 | 15.5 | | 1 | |
| | 1261.426 | 9 | 0.0095 | −0.011 | 11.6 | | 1 | |
| | 1194.614 | 9.02 | 0.0024† | −0.007 | 6.4 | | 1 | |
| | 1193.393 | 11 | 0.008† | −0.012 | 9.1 | | 1 | blend with Si II |
| | 1191.838 | 13 | ... | +0.011 | 5.9 | | 1 | |
| | 1189.631 | 14 | 0.013† | −0.006 | 8.7 | | 1 | |
| | 1189.447 | 14 | 0.0042† | −0.013 | 7.8 | | 1 | |
| | 1158.967 | 15 | ... | −0.027 | 4.1 | | 1 | blend with C I** 15.01 |
| | 1158.397 | 15.01 | 0.003† | −0.004 | 2.5 | | 1 | |
| | 1156.765 | 18.01 | ... | −0.015 | 5.0 | | 1 | |
| | 1156.560 | 19 | 0.016† | −0.009 | 10.9 | | 1 | |
| | 1156.389 | 19 | 0.006† | −0.007 | 7.0 | | 1 | blend with C I* 18.01 |
| | 1123.065 | 26.03 | 0.0001† | +0.007 | 5.2 | | 1 | blend with C I** to $3F^o$ |
| | 1122.33 | 27 | 0.0007† | −0.01 | 7.5 | | 1 | 2 lines |
| | 1122.260 | 27.01 | ... | −0.022 | 9.5 | | 1 | |
| C II..... | 1334.532 | 1 | 0.118 | −0.037 | 189 | 2 | 3 | |
| | 1036.337 | 2 | 0.125 | | | | | blend with $H_2(5,0)$ $R(0)$ |
| C II*..... | 1335.703 | 1 | 0.118 | −0.030 | 140 | 4 | 3 | 2 lines |
| | 1037.018 | 2 | 0.125 | | | | | blend with $H_2(5,0)$ R(1) |
| C IV..... | 1548.202 | 1 | 0.194 | −0.002 | ≤12: | 3§ | 15 | |
| N I..... | 1200.711 | 1 | 0.0442 | −0.039 | 133 | 4 | 5 | |
| | 1200.224 | 1 | 0.0885 | −0.037 | 131 | 1 | 3 | |
| | 1199.549 | 1 | 0.133 | −0.032 | 146 | 3 | 2 | |
| | 1134.980 | 2 | 0.0402 | −0.035 | 126 | 3 | 3 | |
| | 1134.415 | 2 | 0.0268 | −0.035 | 122 | 4 | 3 | |
| | 1134.165 | 2 | 0.0134 | −0.035 | 119 | 3 | 3 | |
| N II ..... | 1083.990 | 1 | 0.101 | −0.022 | 125 | 6 | 3 | |
| N II* ..... | 1084.575 | 1 | 0.101 | ... | 97–25 | 2 | 3 | 2 lines blend with $H_2(2,0)$ $P(3)$ |
| N II** ..... | 1085.701 | 1 | 0.0845 | +0.005 | 35 | 4§ | 1 | |
| | 1085.545 | 1 | 0.0161 | −0.008 | 14.9 | 3.9 | 4 | 2 lines |
| N III..... | 989.790 | 1 | 0.107 | ... | ≤40: | | 1 | blend with Si II, $H_2$ $Q(3)$ |
| N V ..... | 1242.804 | 1 | 0.0757 | ... | < 2.3 | | 1 | |
| | 1238.821 | 1 | 0.152 | ... | < 3.8 | | 1 | |
| O I..... | 1355.598 | 1 | $3.6 \times 10^{-7}$ | −0.010 | ≤10.6 | 5§ | 1 | |
| | 1302.169 | 2 | 0.0485 | −0.038 | 201 | 7 | 4 | asymmetric long $\lambda$ |
| | 1039.230 | 3 | ... | −0.020 | 108 | | 1 | |
| O I*..... | 1304.858 | 2 | 0.0485 | ... | < 3.9 | | 1 | |
| O I**..... | 1306.029 | 2 | 0.0485 | ... | < 4.0 | | 1 | |
| O VI..... | 1037.627 | 1 | 0.0648 | ... | < 11 | | 1 | |
| | 1031.945 | 1 | 0.130 | ... | | | | blend with HD(6,0) $R(0)$ |
| Mg I..... | 2852.127 | 1 | 1.90 | −0.040 | 218 | 12 | 2 | |
| | 2025.824 | 2 | 0.161 | −0.125 | 31: | 5 | 8 | |
| Mg II..... | 2802.704 | 1 | 0.295 | −0.090 | 290 | 11 | 4 | |
| | 2795.528 | 1 | 0.592 | −0.095 | 312 | | 1 | |
| | 1240.395 | | 0.000484 | −0.014 | 13.2 | 0.5 | 2 | |
| | 1239.925 | | 0.000968 | −0.014 | 18.7 | 2.4 | 2 | |
| Al II..... | 1670.786 | 2 | 1.88 | −0.024 | 55: | 11§ | 10 | |
| Al III ..... | 1862.790 | 1 | 0.268 | −0.080 | 34: | | 5 | |
| | 1854.716 | 1 | 0.539 | −0.076 | 57: | | 5 | |
| Si I..... | 2514.316 | 1 | 0.156 | −0.049 | ≤11 | 3§ | 2 | |
| Si II ..... | 1808.012 | 1 | 0.00371 | −0.092 | 87 | 11 | 5 | |
| | 1526.708 | 2 | 0.0764 | +0.030 | 190: | | 4 | |
| | 1304.372 | 3 | 0.147 | −0.041 | 132 | 1 | 2 | |
| | 1260.421 | 4 | 0.959 | −0.032 | 170 | | 1 | blend with Fe II |
| | 1193.289 | 5 | 1.30 | −0.034 | 147 | 2 | 3 | blend with C I |
| | 1190.416 | 5 | 0.650 | −0.031 | 132 | 3 | 5 | |
| | 1020.699 | 5.01 | 0.0482 | −0.016 | 74 | 1 | 2 | blend with $H_2(7,0)$ $R(4)$ |
| | 989.873 | 6 | 0.244 | ... | ≤40: | | 1 | blend with N III, $H_2$ $Q(3)$ |
| Si II* ..... | 1309.277 | 3 | 0.147 | ... | < 4 | | 1 | |
| | 1264.737 | 4 | 0.860 | −0.004 | 15.4 | 3.5§ | 1 | |
| | 1197.394 | 5 | 0.323 | −0.022 | 4.8 | 3.4§ | 1 | |
| | 1194.500 | 5 | 1.62 | −0.010 | 14.3 | 1.6 | 3 | blend with C I** 1194.488 |

TABLE 1—*Continued*

| Ion | $\lambda_{Lab}$ (Å) | Mlt. No. | $f$ | $\lambda_{Obs} - \lambda_{Lab}$ (Å) | $W_\lambda$ (mÅ) | m.e. (mÅ) | No. Obs. | Remarks |
|---|---|---|---|---|---|---|---|---|
| Si III..... | 1206.510 | 2 | 1.66 | −0.022 | 123 | 3 | 3 | asymmetric |
| Si IV..... | 1402.770 | 1 | 0.262 | +0.002: | 17.9 | 3§ | 7 | |
| | 1393.755 | 1 | 0.528 | −0.020: | 24.7 | 3§ | 8 | |
| P II..... | 1301.87 | 2 | 0.0402 | −0.025 | 15.9 | 3.1 | 4 | |
| | 1152.81 | 3 | 0.19: | −0.010 | 61. | | 1 | asymmetric |
| P III..... | 1334.866 | 1 | 0.0321 | ... | < 5.1 | | 1 | |
| P V..... | 1128.006 | 1 | 0.245 | ... | < 3.8 | | 1 | |
| | 1117.979 | 1 | 0.495 | ... | < 3.3 | | 1 | |
| S I ..... | 1807.311 | 2 | 0.112 | −0.074 | 27.8 | 2.7 | 6 | |
| | 1401.541 | 6 | 0.0158 | ... | < 18 | | 1 | |
| | 1316.553 | 8 | 0.041: | +0.005: | 17.8 | | 1 | 3 lines |
| | 1303.430 | ... | 0.016: | ... | < 6 | | 1 | |
| | 1296.174 | 9 | 0.036: | −0.012 | 14.2 | 1.6 | 3 | |
| | 1295.653 | 9 | 0.108: | −0.017 | 15.3 | 1.3 | 3 | |
| | 1270.782 | ... | ... | −0.009 | 8.7 | | 1 | near C I** λ1270.844 |
| S II..... | 1259.520 | 1 | 0.0159 | −0.040 | 112 | 1 | 2 | |
| | 1253.812 | 1 | 0.0107 | −0.038 | 106 | 2 | 2 | |
| | 1250.586 | 1 | 0.00535 | −0.031 | 100 | 3 | 3 | |
| S III ..... | 1190.206 | 1 | 0.0224 | −0.011 | 67 | 2 | 5 | |
| | 1012.504 | 2 | ... | ... | | | | blend with $H_2$(7,0) $R$(0) |
| S IV ..... | 1062.672 | 1 | 0.0377 | ... | | | | blend with $H_2$(3,0) $R$(0) |
| Cl I..... | 1347.240 | 2 | 0.112 | −0.015 | 20.3 | | 1 | |
| | 1188.772 | ... | 0.0881 | −0.017: | 22.7 | | 1 | 2 lines, blend with C I |
| | 1094.769 | ... | ... | −0.006 | 13–15 | | 1 | blend with $H_2$(2,0) $R$(6) |
| | 1097.369 | ... | ... | +0.006 | 10.3 | | 1 | |
| Cl II..... | 1071.036 | 1 | 0.0159 | −0.022 | 4.1 | 2.2§ | 2 | |
| Cl III ..... | 1005.280 | 1 | 0.00717 | ... | < 15 | | 1 | |
| Ar I ..... | 1066.660 | 1 | 0.0594 | −0.023 | 85 | 3 | 3 | |
| | 1048.218 | 2 | 0.230 | −0.019 | 97 | 6 | 2 | |
| Ti III..... | 1298.67 | 1 | 0.0892 | ... | < 2.9 | | 2 | |
| | 1291.64 | 2 | 0.0850 | ... | < 3.7 | | 1 | |
| V II..... | 2683.09 | 3 | 0.071: | ... | < 11 | | 2 | |
| V III..... | 1153.19 | 2 | 0.10‡ | ... | < 2.9 | | 1 | |
| | 1123.55 | 3 | 0.055‡ | ... | < 2.9 | | 1 | |
| Cr II..... | 2055.59 | 1 | 0.17‡ | ... | < 8.3 | | 6 | |
| Cr III ..... | 1033.35 | 2 | 0.052‡ | ... | < 6.8 | | 1 | |
| Mn II..... | 2605.697 | 1 | 0.158 | −0.090 | 111 | 6 | 4 | |
| | 2593.731 | 1 | 0.223 | −0.111: | 116 | 5 | 4 | |
| | 2576.107 | 1 | 0.288 | −0.107 | 138 | 21 | 3 | |
| | 1201.124 | 3 | 0.058† | −0.031: | 12.1 | | 1 | asymmetric |
| | 1199.388 | 3 | 0.10:† | −0.019: | 20.4 | | 1 | in wing of N I λ1199.549 |
| | 1197.172 | 3 | 0.096† | −0.017 | 18.7 | | 1 | |
| Fe II..... | 2599.395 | 1 | 0.203 | −0.106 | 226 | 16 | 3 | |
| | 2585.876 | 1 | 0.0573 | −0.111 | 214 | 19 | 2 | |
| | 2382.034 | 2 | 0.328 | −0.122 | 238 | 20 | 2 | |
| | 2373.733 | 2 | 0.0395 | −0.145 | 120 | 41 | 2 | |
| | 2343.495 | 3 | 0.108 | −0.141 | 186 | 18 | 4 | |
| | 1608.456 | 8 | ... | −0.009 | 85: | | 4 | |
| | 1260.542 | 9 | 0.02† | ... | 38: | | 1 | blend with Si II |
| | 1144.946 | 10 | 0.15† | −0.041 | 91 | | 1 | |
| | 1143.235 | 10 | 0.015† | −0.045 | 38 | | 1 | asymmetric |
| | 1142.334‖ | 10 | 0.0069† | +0.008 | 18.1 | | 1 | asymmetric |
| | 1133.678 | 11 | 0.0063† | −0.048 | 15.7 | | 1 | |
| | 1121.987 | 12 | 0.020† | −0.041 | 42 | | 1 | |
| | 1106.362 | 15 | ... | −0.048 | 14.1# | | 1 | |
| | 1096.886 | 18 | 0.037† | −0.044 | 52 | | 1 | |
| | 1055.269 | 21 | 0.010† | −0.021 | 21.1 | | 1 | |
| Fe II*..... | 2395.627 | 2 | 0.276 | ... | < 11 | | 2 | |
| | 1148.295 | 10 | 0.13† | −0.035 | ≤4.8: | 2.6§ | 1 | |
| Fe III ..... | 1122.526 | 1 | 0.056‡ | −0.010 | 21.3 | 2.6 | 2 | blend with C I λλ1122.518, 1122.447 |
| Co II ..... | 2011.546 | 4 | 0.44‡ | −0.045: | ≤25 | 2§ | 6 | |

TABLE 1—*Continued*

| Ion | $\lambda_{Lab}$ (Å) | Mlt. No. | $f$ | $\lambda_{Obs} - \lambda_{Lab}$ (Å) | $W_\lambda$ (mÅ) | m.e. (mÅ) | No. Obs. | Remarks |
|---|---|---|---|---|---|---|---|---|
| Ni II..... | 1370.136 | 8 | 0.10‡ | −0.041 | 19.7 | 5.7§ | 1 | |
| | 1393.330 | | 0.018‡ | ... | < 9.1 | | 1 | |
| Cu II ..... | 1358.773 | 3 | 0.54‡ | −0.038 | 7.4 | 2.2§ | 6 | |
| Zn II..... | 2062.016 | 1 | 0.202 | −0.160 | 95: | | 8 | |
| | 2025.512 | 1 | 0.412 | −0.154 | 100: | | 8 | |

NOTE.—Vacuum wavelengths are quoted shortward of 2000 Å and air values longward.

* First excited fine-structure state.

** Second excited fine-structure state.

† Estimated $f$-value from *Copernicus* spectra, including ζ Oph.

‡ Theoretical $f$-value from Kurucz (1974).

§ 2 σ error calculated as described by Jenkins *et al.* (1973).

‖ Comparison with other interstellar Fe II lines suggests that the laboratory wavelength of this line is closer to 1142.38 Å.

# According to G. F. Drake and S. R. Pottasch, this Fe II line is absent in ζ Ori A, so that $f < 0.056$ and the line in ζ Oph probably should be listed in table 2 with $\lambda_{obs} = 1106.314$.

The V1 detector was used in first order longward of 1600 Å while the U1 detector was used in second order shortward of 1500 Å and in first order for lines between 1440 and 1610 Å. The instrumental profile is approximately Gaussian with a FWHM of 0.10 Å in first order and 0.05 Å in second order (Spitzer and Morton 1975). Complete V2 scans (0.4 Å FWHM) between 1830 and 3120 Å have shown that there are no strong interstellar features not covered by the higher resolution V1 scans of selected lines. During the 1973 and 1974 U1 scans, the dipping mirror on the low-resolution carriage was positioned to occult the outgassing holes near the U1 exit slit to eliminate the stray light described by York *et al.* (1973). Whether or not these holes were covered, the U1 background levels were obtained by interpolating between the flat bottoms of the many strong interstellar absorption lines. In the case of V1, the corrections for the counts due to energetic particles were derived from measurements near the same magnetic longitude and latitude with no star signal reaching the tube.

Altogether about 370 different interstellar lines were found. Equivalent widths were obtained for 72 due to $H_2$, 6 due to HD, 11 due to CO, 82 due to C I, and 81 from the remaining atoms and ions listed in table 1. The unidentified lines in table 2 total 45. Another 46

TABLE 2

UNIDENTIFIED INTERSTELLAR LINES IN ζ OPHIUCHI

| $\lambda_{obs}$ (Å) | $W_\lambda$* (mÅ) | Blends and Rejected Identifications | $\lambda_{obs}$ (Å) | $W_\lambda$* (mÅ) | Blends and Rejected Identifications |
|---|---|---|---|---|---|
| 1006.418 ..... | 55. | blend with $H_2$(9,0) $P$(5), Cl I | 1107.035 ..... | 5.1 | |
| 1017.003 ..... | 28.7 | $H_2$(0,0) $R$(6) | 1107.135 ..... | 8.5 | |
| 1021.210 ..... | 15.3 | $H_2$(0,0) $Q$(6) | 1107.345 ..... | 7.2 | |
| 1031.832 ..... | 5.7 | O VI λ1031.945 | 1109.035 ..... | 17.6 | |
| 1043.275 ..... | 6.5 | HD(5,0) $R$(1) | 1109.620 ..... | 16.3 | |
| 1055.545 ..... | 4.2 | HD(4,0) $P$(1) | 1110.433 ..... | 12.7 | |
| 1059.476 ..... | 14.0 | | 1111.414 ..... | 17.0 | |
| 1081.850† ..... | 31. | | 1111.650 ..... | 10.5 | |
| 1088.000† ..... | 48. | CO(0,0) $P$(1,2,3), Cl I | 1112.028 ..... | 22.5 | $H_2$(3,1) $R$(0), C I** |
| 1101.008 ..... | 6.9 | $H_2$(2,0) $R$(7) | 1112.240 ..... | 21.3 | |
| 1103.623 ..... | 19.7 | asymmetric | 1113.770 ..... | 13.1 | |
| 1103.834 ..... | 9.3 | | 1114.633 ..... | 18.6 | |
| 1104.430 ..... | 7.2 | | 1114.872 ..... | 9.3 | |
| 1104.628 ..... | 6.3 | | 1117.870 ..... | 14.7 | |
| 1104.772 ..... | 9.0 | | 1121.435 ..... | 9.2 | blend with C I 27.03 |
| 1104.947 ..... | 12.7 | | 1121.652 ..... | 8.7 | blend with C I 27.01 |
| 1105.195 ..... | 9.6 | | 1125.415† ..... | 39. | |
| 1105.519 ..... | 10.8 | asymmetric | 1127.082 ..... | 10.9 | |
| 1105.708 ..... | 14.7 | | 1156.273 ..... | 12.1 | |
| 1105.822 ..... | 13.6 | HD(0,0) $R$(0) | 1159.370 ..... | 5.4 | |
| 1105.916 ..... | 3.8 | | 1308.087 ..... | 9.2 | |
| 1106.240 ..... | 6.0 | | 1317.140 ..... | 19.0 | |
| 1106.508 ..... | 5.3 | | | | |

* All lines scanned only once except λ1103.834 for which the mean error in $W_\lambda$ is 1.7 mÅ.

† Unidentified lines at similar wavelengths in several other stars.

$H_2$ lines were too strong or sufficiently blended to permit the direct determination of equivalent widths and 27 blended C I lines were omitted from table 1. The C I lines represent almost all the transitions between 1562 and 1111 Å listed by Moore (1970*a*), as well as a few from Kelly and Palumbo (1973). Some of the unidentified lines in table 2 between 1115 Å and the ionization limit at 1101.074 Å also could be C I.

Laboratory wavelengths, ultraviolet multiplet numbers, *f*-values, and radiation damping constants were obtained mainly from the list of Morton and Smith (1973). Improved wavelengths for B II, Al III, Si II, S I, Cl I, Ni II, and Cu II were taken from Kelly and Palumbo (1973), and for Cl II from Radziemski and Kaufman (1974). The majority of the oscillator strengths were based on measurements or detailed

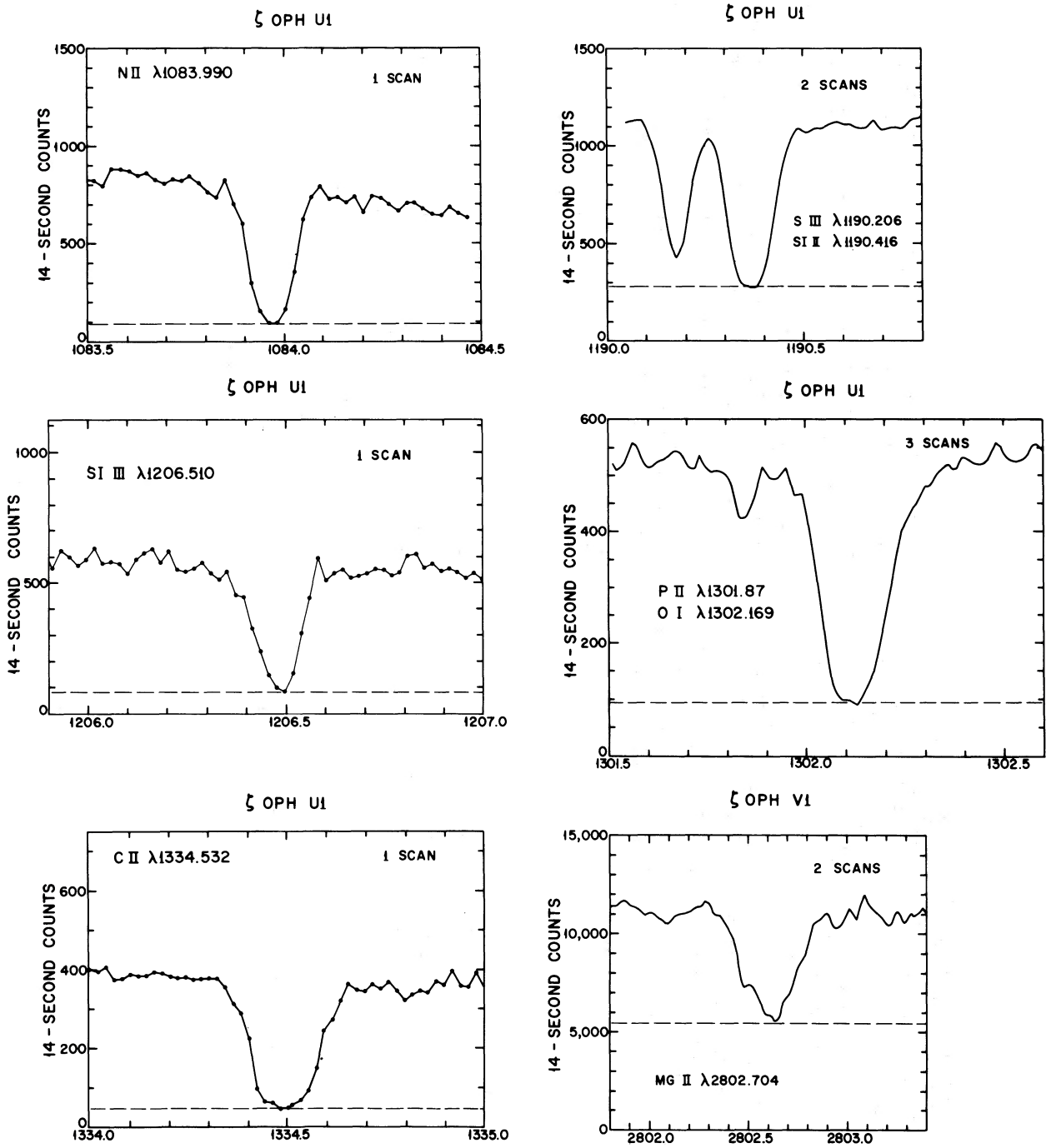


FIG. 1.—Profiles of some of the stronger interstellar lines in the ζ Oph spectrum. The horizontal dashed line indicates the adopted zero level. In three cases the plot resulted from the stacking of multiple scans.

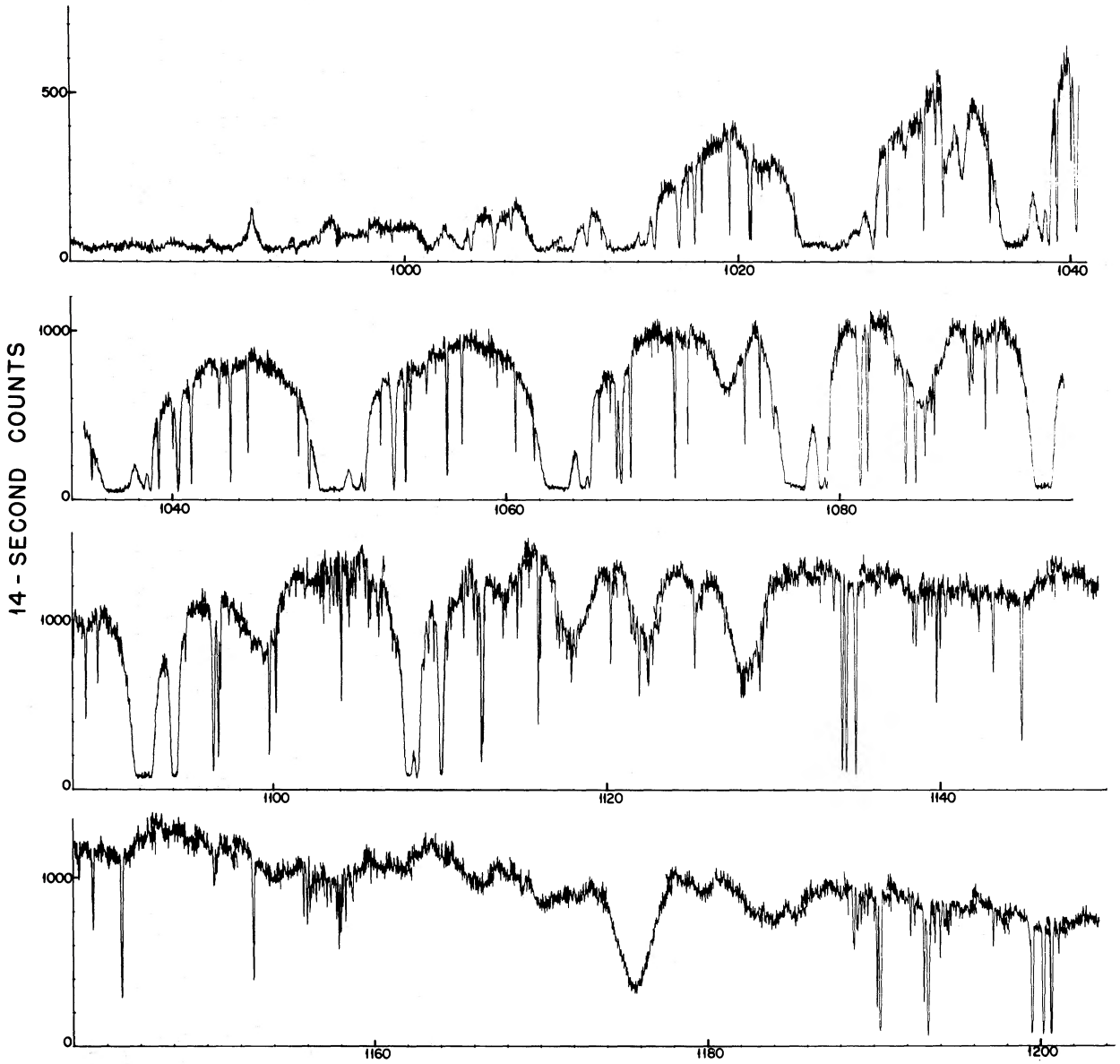


FIG. 2*a*.—The spectrum of ζ Oph from 980 to 1204 Å. No corrections have been applied for the spectrometer sensitivity, the amount of light entering the slit, scattered light from the grating, or counts from energetic particles. Consequently the star signal is weak at the shortest wavelength, there are discontinuities between some scans, and the bottoms of the saturated interstellar lines are not at zero. The broad relatively shallow stellar features are easily distinguishable from the interstellar lines which are either very sharp or wide and saturated, as is the case for the strongest $H_2$ lines.

calculations, with some approximate values added for V III, Cr II, Cr III, Fe III, Co II, Ni II, and Cu II from calculations by Kurucz (1974). Also a number of *f*-values for C I, Mn II, and Fe II have been estimated by de Boer and Morton (1975) and de Boer *et al.* (1974) using *Copernicus* spectra, including ζ Oph. Absorptions from excited fine-structure levels are indicated by asterisks. In both tables 1 and 2, there are still some errors in the scale for observed wavelengths so that the quantities $\lambda_{obs} - \lambda_{lab}$ and $\lambda_{obs}$ can be trusted only in a relative way. Also there has been no attempt to fit together the separate scales for λλ980–1420 (U1 2nd order), λλ1440–1610 (U1 1st order), or λλ1670–2860 (V1 1st order). The equivalent widths normally are listed with mean errors when duplicate scans were available and uncertain values are indicated by a colon. The lines noted as asymmetric usually have the additional absorption in the short-wavelength wing, though it is in the long-wavelength wing of λ1302 of O I (see fig. 1). In these cases the observed wavelength was measured at the deepest part of the profile. Table 1 also contains upper limits (designated by <) for the

equivalent widths of 22 lines determined according to the principles for a 2 $\sigma$ limit described by Jenkins *et al.* (1973).

A line observed at 1084.563 Å with $W_\lambda = 97 \pm 2$ mÅ is a blend of $H_2(2,0)\,P(3)$ λ1084.559 and N II* λλ1084.580, 1084.562. The curve of growth for the $H_2$ lines with $J'' = 3$ showed that $W_\lambda(H_2) = 72$ mÅ so that $W_\lambda$(N II*) must be between 25 and 97 mÅ depending on the amount of saturation. Similarly, the contribution of $H_2(2,0)\,R(6)$ λ1094.794 to a blend at 1094.763 Å with $W_\lambda = 15.1$ mÅ was estimated to be about 2.4 mÅ, leaving $12.7 \leq W_\lambda \leq 15.1$ for Cl I λ1094.769. A blend due to $H_2(1,0)\,Q(3)$ λ989.727, N III λ989.790, and Si II λ989.873 produced a single asymmetric line having $W_\lambda = 125$ mÅ with the deepest part centered at 989.712 Å and an additional contribution on the long-wavelength side. It appears that $H_2$ is the major component, with no more than 40 mÅ attributable to either N III or Si II. Lines due to C IV λ1548.2, Si I λ2514.3, Fe II* λ1148.3, and Co II λ2011.5 probably are present with the listed values of $W_\lambda$ (designated by $\leq$), but the detections were not conclusive so that the analyses were based on only upper limits equal to $W_\lambda + 2\,\sigma$.

Smith (1972) was the first to find the interstellar lines of C I, C II, C II*, O I, Si II, and S II in the ultra-

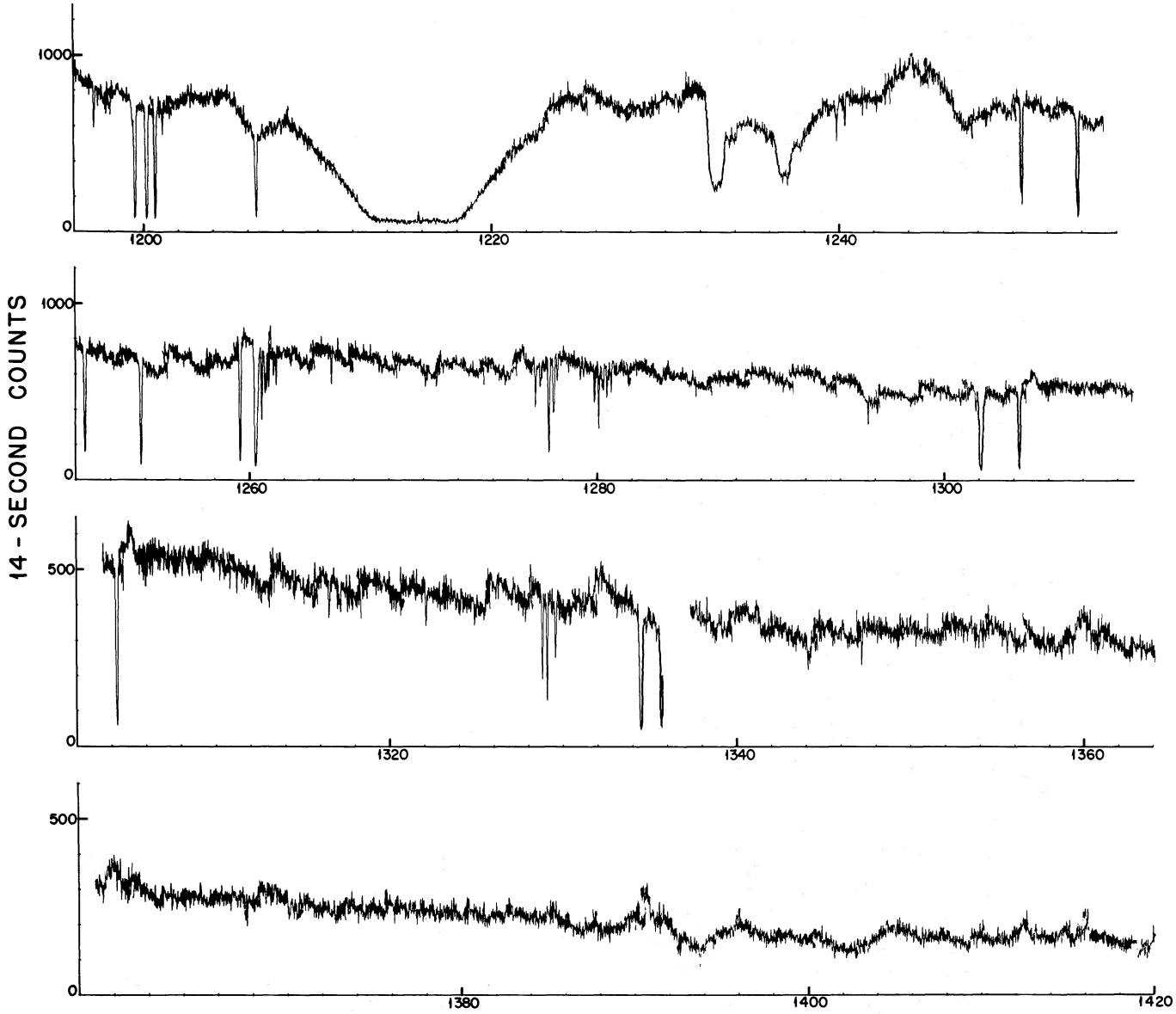


FIG. 2*b*.—The spectrum of ζ Oph from 1196 to 1420 Å, again without the corrections described under fig. 1*a*. Here the guidance variations during each scan frequently caused changes in the continuum level which could be mistaken for features in the stellar spectrum. The Lα airglow emission is visible at the center of the wide interstellar absorption line.

violet spectrum of ζ Oph. His equivalent widths exceed the *Copernicus* measures by about 40 percent in the mean, while Jenkins's (1973) values average 80 percent high.

Figure 1 gives the profiles of several of the interstellar lines, with multiple scans added together in some cases. Figure 2 is a compressed plot of many adjoining high-resolution scans. The depression of the continuum at short wavelengths by the $H_2$ bands is particularly striking. The N v P-Cygni lines are visible longward of the interstellar Lα absorption. The centers of the displaced absorption lines correspond to a mass outflow of 1420 km s$^{-1}$, and the short-wavelength edge is at 1550 km s$^{-1}$.

### *b) Visible and Near-Ultraviolet Lines*

Table 3 has been compiled from the ground-based observations of several authors along with the wavelengths and *f*-values of Morton and Smith (1973). Herbig (1968), Shulman *et al.* (1974), and Lutz (1974) used photographic spectra from the Lick Observatory, while Hobbs (1973*a*) and Traub and Carleton (1973) used Fabry-Perot interferometers, and White (1973) used a scanning spectrometer. The photographic equivalent widths agree among themselves within 0.7 mÅ or less for the Ca II lines and even better with White's measurement of Ca I. In most cases, the more comprehensive photographic data have been preferred for the means in the table, but it should be noted that Hobbs found $W_\lambda = 169$ mÅ for the four components of Na I λ5896 near −14 km s$^{-1}$, where the correction for parasitic light should be well known. The $W_\lambda$ for K I λ7699 is the mean of 97 mÅ from Herbig, 76 mÅ from Hobbs, and 80 mÅ from Lutz. When interferometer profiles were available, they were used for the heliocentric radial velocities. The velocities of Na I, K I, and Ca II from Herbig and from Shulman, Bortolot, and Thaddeus were corrected to the wavelengths in column (2), which were measured by Risberg (1956) or Edlén and Risberg (1956).

The lower resolution spectra show that the strongest absorptions of Na I and Ca II occur near a heliocentric velocity $V_\odot = -15$ km s$^{-1}$ with weaker lines around −28 km s$^{-1}$. Hobbs (1973*a*) found that each of these features contains partially resolved components with velocities of −9.0, −12.6, −14.4, −17.5, −25.5, and −27.6 km s$^{-1}$. The largest fractions of Na I and Ca II appear to be divided between the clouds at −14.4 and −12.6 km s$^{-1}$, but all the detectable K I is at −14.4

TABLE 3

VISIBLE ATOMIC INTERSTELLAR LINES IN ζ OPHIUCHI

| Ion | $\lambda_{lab}$(air) (Å) | Mlt. No. | *f* | Radial Velocity (km s$^{-1}$) | R* | $W_\lambda$ (mÅ) | R* |
|---|---|---|---|---|---|---|---|
| Li I..... | 6707.912 | 1 | 0.251 | −14.9 | 4 | 0.68 | 4 |
| | 6707.761 | 1 | 0.502 | | | | |
| Be II..... | 3130.064 | 1 | 0.169 | | | < 2.5 | 1 |
| Na I..... | 5895.924 | 1 | 0.327 | −10,0, −12.6, −14.4, −17.5 | 2 | 189 | 1 |
| | | | | −25.5, 27.6 | 2 | 21.5 | 1,2 |
| | 5889.950 | 1 | 0.655 | −10.0, −12.6, −14.4, −17.5 | 2 | 239 | 1 |
| | | | | −25.5, −27.6 | 2 | 27.2 | 1,2 |
| | 3302.979 | 2 | 0.0067 | −13.7 | 1 | 22.3 | 1 |
| | 3302.369 | 2 | 0.0134 | −14.0 | 1 | 28.7 | 1 |
| Al I ..... | 3944.006 | 1 | 0.117 | | | < 0.26 | 5 |
| K I..... | 7698.959 | 1 | 0.339 | −14.4 | 2 | 84 | 1,2,7 |
| | 4047.206 | 3 | 0.00304 | −14.5 | 5 | 0.3 | 5 |
| | 4044.136 | 3 | 0.00609 | −14.6 | 5 | 0.8 | 5 |
| Ca I..... | 4226.728 | 2 | 1.61 | −15.8 | 5 | 1.30 | 3,5 |
| | | | | ~ −28 | | < 0.33 | 3 |
| Ca II..... | 3968.468 | 1 | 0.341 | −14.3 | 1,5 | 21.0 | 1,5 |
| | | | | −28.2 | 1,5 | 5.0 | 1,5 |
| | 3933.663 | 1 | 0.688 | −10.0, −12.6, −14.4, −17.5 | 2 | 34.5 | 1,5 |
| | | | | −27.6 | 2 | 10.0 | 1,5 |
| Ti I..... | 3635.462 | 19 | 0.170 | | | < 3 | 1 |
| Ti II..... | 3383.761 | 1 | 0.332 | ~ −15 | | < 3 | 1 |
| | | | | −27.3 | 1 | 6.9 | 1 |
| | 3241.984 | 2 | 0.203 | −26.3 | 1 | 5.9 | 1 |
| | 3229.193 | 2 | 0.0614 | | | < 3† | 1 |
| | 3072.971 | 5 | 0.109 | | | < 3 | 1 |
| V I..... | 3183.982 | 14 | 0.343 | | | < 3 | 6 |
| Cr I..... | 3593.488 | 4 | 0.255 | | | < 3 | 6 |
| Mn I..... | 4030.755 | 2 | 0.0611 | | | < 3 | 1 |
| Fe I..... | 3859.913 | 4 | 0.0286 | −15.0 | 5 | 1.0 | 5 |
| | 3719.935 | 5 | 0.0413 | −14.9 | 5 | 1.9 | 5 |
| Co I..... | 3474.018 | 4 | 0.00185 | | | < 3 | 1 |
| Ni I..... | 3369.573 | 6 | 0.0195 | | | < 3 | 6 |
| Cu I..... | 3247.540 | 1 | 0.440 | | 1 | < 3 | 1 |

* REFERENCES. (1) Herbig 1968; (2) Hobbs 1969*a*, 1973*a*; (3) White 1973; (4) Traub and Carleton 1973; (5) Shulman *et al.* 1974; (6) Herbig 1974; (7) Lutz 1974.

† Line is present in −28 km s$^{-1}$ cloud.

while all the $CH^+$ is at $-12.6$ km s$^{-1}$. The Ti II lines so far have been found only near $V_\odot = -28$ km s$^{-1}$. The weak lines of Li I, Ca I, and Fe I probably arise in the cloud stationary with respect to the local standard of rest would have $V_\odot = -13.9$ km s$^{-1}$. Herbig (1968) and Hobbs (1969*b*) have noted that at least seven stars across 15° of sky in Ophiuchus, Scorpius, and Libra have a similar pattern of Ca II lines with one set near zero velocity and a weaker set near $-15$ km s$^{-1}$ relative to the local standard of rest.

According to Grayzeck and Kerr (1974) the 21-cm emission from the direction of $\zeta$ Oph has peak intensity at $V_\odot = -12.2$ with a significant shoulder extending to $-14.5$ km s$^{-1}$. The profile drops steeply at more negative velocities to an extended tail which could include contributions from the clouds at $V_\odot = -25.5$ and $-27.6$ km s$^{-1}$. Similar profiles have been described by Hobbs (1971) from observations of Goldstein and MacDonald (1969).

Georgelin and Georgelin (1970) reported a heliocentric radial velocity of $-8.0$ km s$^{-1}$ for the H$\alpha$ emission from the H II region around $\zeta$ Oph. Therefore none of the absorption components, except possibly the weak contributions to Na I and Ca II at $-9.0$ km s$^{-1}$, can originate in the Strömgren sphere. The H$\alpha$ velocity is consistent with the stellar radial velocity of $-10.7 \pm 3.7$ (p.e.) km s$^{-1}$ (Lesh 1968).

### c) *Molecules*

Equivalent widths for many of the $H_2$ Lyman lines in $\zeta$ Oph are listed in table 4, which extends the data presented by Spitzer *et al.* (1974). Additional lines are noted where blending or extensive damping wings have prevented the direct measurement of the equivalent width. J. F. Drake is preparing an analysis of the strong $R(0)$, $R(1)$, and $P(1)$ lines by fitting profiles. The $H_2$ wavelengths were obtained from the measurements of Wilkinson (1968) and Dabrowski and Herzberg (1974*a*) or from calculations by G. M. Lawrence (private communication). Absorption lines from the excited rotational levels of the lowest vibrational level are prevalent in $\zeta$ Oph, but there is no evidence for excited vibrational levels. A search for Werner lines revealed strong absorptions due to (0,0) $R(0)$, $R(1)$, and $Q(2)$ between 1008 and 1010 Å and the

TABLE 4

INTERSTELLAR $H_2$ LYMAN LINES IN $\zeta$ OPH*

$B\ ^1\Sigma_u^+ - X\ ^1\Sigma_g^+$

| | | | R(0) | R(1) | P(1) | R(2) | P(2) | R(3) | P(3) | R(4) | P(4) | R(5) | P(5) | R(6) | P(6) |
|---|---|---|---|---|---|---|---|---|---|---|---|---|---|---|---|
| $g_\ell$ | | | 1 | 9 | 9 | 5 | 5 | 21 | 21 | 9 | 9 | 33 | 33 | 13 | 13 |
| E.P.$_\ell$(cm$^{-1}$) | | | 0.0 | 118.49 | 118.49 | 354.39 | 354.39 | 705.54 | 705.54 | 1168.83 | 1168.83 | 1740.25 | 1740.25 | 2415.06 | 2415.06 |
| v' | v" | | | | | | | | | | | | | | |
| 0 | 0 | λ | 1108.128 | 1108.634 | 1110.063 | 1110.120 | 1112.495 | 1112.584 | 1115.896 | 1116.013 | 1120.247 | 1120.399 | 1125.539 | 1125.725 | 1131.752 |
| | | $W_\lambda$ | p | p | p | p | pR(3) | pP(2) | 50 | 27.3 | 29.7 | 5.6 | 4.8 | | |
| 1 | 0 | λ | 1092.194 | 1092.732 | 1094.052 | 1094.244 | 1096.439 | 1096.725 | 1094.788 | 1100.165 | 1104.084 | 1104.547 | 1109.313 | 1109.859 | 1115.453 |
| | | $W_\lambda$ | p | p | p | p | 166 | 75 | 78 | 35 | 45 | 14.2 | 22.5 | | |
| 2 | 0 | λ | 1077.138 | 1077.698 | 1078.925 | 1079.226 | 1081.265 | 1081.710 | 1084.559 | 1085.144 | 1088.794 | 1089.512 | 1093.955 | 1094.794 | 1100.016 |
| | | $W_\lambda$ | p | p | p | 131 | 202 | 73 | pNII* | 43 | 43 | 27.3 | pP(1) | CII | 7.5: |
| 3 | 0 | λ | 1062.883 | 1063.461 | 1064.606 | 1064.995 | 1066.901 | 1067.480 | 1070.142 | 1070.898 | 1074.313 | 1075.244 | 1079.399 | 1080.492 | 1085.382 |
| | | $W_\lambda$ | p | p | p | 200 | 312 | 80 | 80 | 48 | 43 | 35 | 24.5 | 3.0: | 3.2: |
| 4 | 0 | λ | 1049.368 | 1049.961 | 1051.034 | 1051.499 | 1053.281 | 1053.976 | 1056.469 | 1057.379 | 1060.580 | 1061.697 | 1065.598 | 1066.909 | 1071.497 |
| | | $W_\lambda$ | p | p | p | 228 | 267 | 105 | 79 | 50 | 44 | 40 | 29.3 | pP(2) | 3.9: |
| 5 | 0 | λ | 1036.546 | 1037.150 | 1038.156 | 1038.690 | 1040.367 | 1041.156 | 1043.498 | 1044.546 | 1047.554 | 1048.835 | 1052.499 | 1053.978 | 1058.319 |
| | | $W_\lambda$ | p | p | p | 222 | 290 | 78 | 82 | 48 | 44 | R(0) | 28.1 | pR(3) | |
| 6 | 0 | λ | 1024.364 | 1024.986 | 1025.935 | 1026.532 | 1028.106 | 1028.986 | 1031.191 | 1032.356 | 1035.184 | 1036.546 | 1040.062 | 1041.728 | 1045.805 |
| | | $W_\lambda$ | p | p | p | p | 415 | 86 | 82 | 57 | 50 | R(0) | 32 | 7.4 | |
| 7 | 0 | λ | 1012.822 | 1013.434 | 1014.334 | 1014.977 | 1016.472 | 1017.428 | 1019.506 | 1020.768 | 1023.437 | 1024.991 | 1028.250 | 1030.072 | 1033.921 |
| | | $W_\lambda$ | p | p | p | 218 W | 227 | 115.W | 80 | 74.W | 58 | R(1) | 32 | | |
| 8 | 0 | λ | 1001.826 | 1002.457 | 1003.304 | 1003.989 | 1005.397 | 1006.418 | 1008.392 | 1009.721 | 1012.261 | 1014.245 | 1017.009 | 1020.875 | 1023.158 |
| | | $W_\lambda$ | | | p | 232 | 233 | | W R(1) | | R(0) | P(1) | | | |
| 9 | 0 | λ | 991.394 | 992.022 | 992.813 | 993.549 | 994.876 | 995.975 | 997.829 | 999.273 | 1001.659 | 1003.431 | 1006.344 | 1008.415 | 1011.871 |
| | | $W_\lambda$ | | p | p | | 100.W | 60 | 52 | 42 | | P(1) | p | P(3) | |

Notes: λ is laboratory wavelength with calculated values indicated by the underline.

$W_\lambda$ is equivalent width in mÅ

p indicates the line is present, but $W_\lambda$ was not measured due to wide wings or blending. The source of the blend is noted in some cases.

W indicates there may be some contribution from a Werner line

TABLE 5

ULTRAVIOLET MOLECULAR LINES IN ζ OPHIUCHI

| Molecule | Transition | $\lambda_{lab}$* (Å) | $f$ | $W_\lambda$ (mÅ) | No. Obs. |
|---|---|---|---|---|---|
| $H_2$ ..... | $C\,^1\Pi_u^{\pm}-X\,^1\Sigma_g^+$ | | | | |
| | (0,0) $Q(2)$ | 1010.941 | 0.0238 | 210 | 1 |
| | (0,0) $R(3)$ | 1010.132 | 0.0170 | 192 | 1 |
| | (0,0) $R(4)$ | 1011.817 | 0.0158 | 38 | 1 |
| | (0,0) $Q(5)$ | 1017.836 | 0.0236 | 40 | 1 |
| | (1,0) $P(2)$ | 989.082 | 0.00726 | 49: | 1 |
| | (1,0) $Q(3)$ | 989.727 | 0.0363 | ≤125: | 1 |
| | (1,0) $P(5)$ | 997.640 | 0.00720 | 48: | 1 |
| HD ..... | $B\,^1\Sigma_u^+-X\,^1\Sigma_g^+$ | | | | |
| | (3,0) $R(0)$ | 1066.271 | 0.0114 | 14.3 | 1 |
| | (4,0) $R(0)$ | 1054.286 | 0.0161 | 19.5 | 1 |
| | (5,0) $R(0)$ | 1042.847 | 0.0200 | 24.6 | 1 |
| | (6,0) $R(0)$ | 1031.909 | 0.0228 | 21.2 | 1 |
| | (7,0) $R(0)$ | 1021.453 | 0.0242 | 14.4 | 1 |
| | (8,0) $R(0)$ | 1011.457 | 0.0244 | 13.9 | 1 |
| | (4,0) $R(1)$ | 1054.727 | 0.0107 | < 3.1 | 1 |
| CO..... | $A\,^1\Pi-X\,^1\Sigma^+$ | | | | |
| | (3,0) | 1447.359 | 0.0360 | 63: | 4 |
| | (4,0) | 1419.044 | 0.0251 | 66 | 1 |
| | (5,0) | 1392.529 | 0.0155 | 68 | 1 |
| | (6,0) | 1367.617 | 0.00848 | 28.3 | 1 |
| | (7,0) | 1344.184 | 0.00437 | 40 | 1 |
| | (8,0) | 1322.147 | 0.00217 | 17.2 | 1 |
| | (9,0) | 1301.401 | 0.00108 | 17.9 | 1 |
| | (10,0) | 1281.866 | 0.0050 | 9.8 | 1 |
| CO..... | $B\,^1\Sigma^+-X\,^1\Sigma^+$ | | | | |
| | (0,0) | 1150.48 | 0.015 | 35 | 1 |
| | $C\,^1\Sigma^+-X\,^1\Sigma^+$ | | | | |
| | (0,0) | 1087.867 | 0.163 | 44 | 1 |
| | $E\,^1\Pi-X\,^1\Sigma^+$ | | | | |
| | (0,0) | 1076.033 | 0.094 | 51 | 3 |
| $^{13}C^{16}O$..... | $A\,^1\Pi-X\,^1\Sigma^+$ | | | | |
| | (5,0) | 1395.3 | 0.0155 | < 7.2 | 1 |
| | (6,0) | 1370.7 | 0.00848 | < 5.7 | 1 |
| OH..... | $D\,^2\Sigma^--X\,^2\Pi$ | | | | |
| | (0,0)$P_1(3/2)$ | 1222.524 | 0.03† | < 4.2 | 3 |
| | (0,0)$Q_1(3/2)$ | 1222.071 | 0.05† | < 5.8 | 3 |
| | (0,0)$R_1(3/2)$ | 1221.166 | 0.02† | < 5.8 | 3 |
| HCl..... | $C\,^1\Pi-X\,^1\Sigma^+$ | | | | |
| | (0,0)$R(0)$ | 1290.257 | 0.05† | < 3.9 | 1 |
| | (1,0)$R(0)$ | 1247.079 | | < 3.6 | 1 |
| $C_2$..... | $F\,^1\Pi_u-X\,^1\Sigma_g^+$ | | | | |
| | (0,0) $R(0)$ | 1341.63 | 0.1† | < 5.2 | 1 |
| $NO^+$ ..... | $A\,^1\Pi-X\,^1\Sigma^+$ | | | | |
| | (0,0) $R(0)$ | 1368.23 | 0.00025 | < 5.7 | 1 |
| | (2,0) $R(0)$ | 1312.94 | 0.0017 | < 2.3 | 3 |
| SiO..... | $J\,^1\Pi-X\,^1\Sigma^+$ | | | | |
| | | 1310.01 | 0.1† | < 3.7 | 1 |
| $H_2O$..... | $3p\,^1\tilde{B}_1-X\,^1\tilde{A}_2$ | | | | |
| | | 1239.73 | 0.15† | < 3.5 | 1 |
| | | 1192.72 | 0.05† | < 3.5 | 1 |

* Vacuum wavelengths.

† Estimated $f$-value.

weaker lines in table 5. Additional lines shortward of 1072 Å in table 2 may belong to the Werner system, but accurate laboratory wavelengths were not available for $J'' > 5$.

The HD wavelengths in table 5 were measured by Dabrowski and Herzberg (1974*b*) and the $f$-values were obtained from Allison and Dalgarno (1970). The (6,0) $R(0)$ line of HD at λ1031.909 nearly coincides with λ1031.945 of O VI. Since the other HD lines are of comparable strength, and there is no evidence for the weaker component of O VI at λ1037.627, the observed feature at λ1031.9 is assumed to be entirely HD. Some weak depressions in the spectrum coincide with $R(1)$ and $P(1)$ wavelengths, but the absence of HD(4,0) $R(1)$ gives an upper limit for the excited molecule.

The electronic transitions of CO are represented by 10 lines in table 5. Most of the features are double, probably due to absorptions from excited rotational levels as well as the $R(0)$ lines, for which the wavelengths are quoted from Simmons, Bass, and Tilford (1969). The $f$-values, which apply to the sum over all

TABLE 6

VISIBLE MOLECULAR INTERSTELLAR LINES IN ζ OPHIUCHI

| Molecule | Transition | $\lambda_{lab}$(air) (Å) | Radial Velocity (km s$^{-1}$) | R* | $W_\lambda$ (mÅ) | R* |
|---|---|---|---|---|---|---|
| CH..... | $A\,^2\Delta - X\,^2\Pi$ | | | | | |
| | (0,0) $J'' = 1/2$ | 4300.321 | −14.6 | 1 | 20.8 | 3 |
| | (0,0) $J'' = 3/2$ | 4303.947 | | | < 0.44 | 3 |
| | $B\,^2\Sigma^- - X\,^2\Pi$ | | | | | |
| | (0,0) $J'' = 1/2$ | 3890.213 | −14.3 | 1 | 5.6 | 1 |
| | (0,0) $J'' = 1/2$ | 3886.410 | −14.4 | 1 | 5.9 | 1 |
| | (0,0) $J'' = 1/2$ | 3878.768 | −13.3 | 1 | 3: | 1 |
| | $C\,^2\Sigma^+ - X\,^2\Pi$ | | | | | |
| | (0,0) $J'' = 1/2$ | 3146.01 | −15.4 | 1 | 5.0 | 1 |
| | (0,0) $J'' = 1/2$ | 3143.15 | −12.5 | 1 | 7.4 | 1 |
| | (0,0) $J'' = 1/2$ | 3137.53 | −13.0: | 1 | 4.0 | 1 |
| $CH^+$ ..... | $A\,^1\Pi - X\,^1\Sigma^+$ | | | | | |
| | (0,0) $R(0)$ | 4232.539 | −14.0<br>−12.6 | 1<br>4 | 22.3 | 5 |
| | (1,0) $R(0)$ | 3957.700 | −15.4 | 1 | 14.0 | 1,6 |
| | (2,0) $R(0)$ | 3745.310 | −15.1 | 1 | 7.2 | 1 |
| | (3,0) $R(0)$ | 3579.020 | | | 3.7 | 1 |
| | (4,0) $R(0)$ | 3447.075 | | | 1–2: | 1 |
| | (0,0) $R(1)$ | 4229.337 | | | < 0.59 | 2 |
| $C^{13}H^+$..... | $A\,^1\Pi - X\,^1\Sigma^+$ | | | | | |
| | (0,0) $R(0)$ | 4232.28 | | | 0.35 | 5 |
| CN..... | $B\,^2\Sigma^+ - X\,^2\Sigma^+$ | | | | | |
| | (0,0) $N'' = 0$ | 3874.608 | −14.8 | 1 | 8.40 | 3 |
| | (0,0) $N'' = 1$ | 3875.763 | −14.9 | 1 | 1.49 | 3 |
| | (0,0) $N'' = 1$ | 3873.998 | −13.8 | 1 | 2.74 | 3 |
| | (0,0) $N'' = 2$ | 3873.369 | | | < 0.43 | 3 |

* REFERENCES.—(1) Herbig 1968; (2) Bortolot and Thaddeus 1969; (3) Bortolot *et al.* 1969; (4) Hobbs 1972, 1973*a*, *b*; (5) Vanden Bout 1972; (6) Yoshimine *et al.* 1973.

rotational levels, were obtained from Lassettre and Skerhele (1971) rather than Pilling, Bass, and Braun (1971), whose numbers are smaller by about a factor 0.6. Solomon (1974) has detected CO emission at 2.6 mm from the direction of ζ Oph, making this molecule the first one to be observed at both ratio and optical wavelengths in the same cloud. He found a heliocentric velocity of −14.1 km s$^{-1}$, indicating that the CO must be present mainly in the cloud where several of the neutral atoms are plentiful. According to Black and Dalgarno (1973*a*), CO can be formed where $H_2$ and $H^+$ are available, so that it is reasonable to assume that the $H_2$ also is in the cloud at −14.4 km s$^{-1}$.

None of the remaining molecules in table 5 were detected, but useful upper limits on $W_\lambda$ were obtained. The results for OH were provided by Larach (1973), with wavelengths from Douglas (1974). The wavelengths for HCl were taken from Tilford, Ginter, and Vanderslice (1970), and the *f*-value was based on the measurements of Myer and Samson (1970), who had to adopt rough estimates for some *f*-values when nothing else was available.

The published data on the visible and near UV molecular lines are summarized in table 6. Herbig (1968) also reported upper limits for OH, NH, MgH, SiH, and $CO^+$. His heliocentric velocities for CH, $CH^+$, and CN average −14.1 ± 0.8, −14.8 ± 0.6, and −14.5 ± 0.5 (m.e.) km s$^{-1}$, respectively, while Hobbs (1973*a*) found that λ4232.539 of $CH^+$ appeared as a single component centered on −12.6 km s$^{-1}$. It is important to settle whether the $CH^+$ has the same velocity as the CO and CH since Black and Dalgarno (1973*b*) and Watson (1974) have argued that $CH^+$ cannot exist in significant quantity in the presence of CH and $H_2$.

Authors also have differed on the equivalent width of the (0,0) $R(0)$ $CH^+$ line. Herbig (1968) found $W_\lambda = 27.4$ mÅ, consistent with Bortolot, Clauser, and Thaddeus (1969), while photoelectric scans by Vanden Bout (1972) and Barker (Hobbs 1973*b*) gave 22.3 and 18.3, respectively, compared with Hobbs's value of 18.9 mÅ. In the case of the corresponding $^{13}CH^+$ line, Vanden Bout measured 0.35 ± 0.10, in agreement with Hobbs's (1972) upper limit of 0.4, but somewhat smaller than the detection by Bortolot and Thaddeus (1969) at 0.63 ± 0.14 mÅ.

## III. RELATIVE VELOCITIES OF CLOUDS AND H II REGIONS

### *a) Far-Ultraviolet lines*

Figure 3 is a plot of the difference between observed and laboratory wavelengths for most of the identified lines recorded in the one continuous U1 scan. Only lines with serious blending or weak lines with uncertain centers have been omitted. Since systematic errors remain in the adopted wavelength scale and thermal drifts with time are possible, these data can be used for only relative velocities. However, the internal consistency of various groups of points indicates that differences at a given wavelength probably are reliable to ±0.01 Å. Furthermore, the geocoronal Lα emission

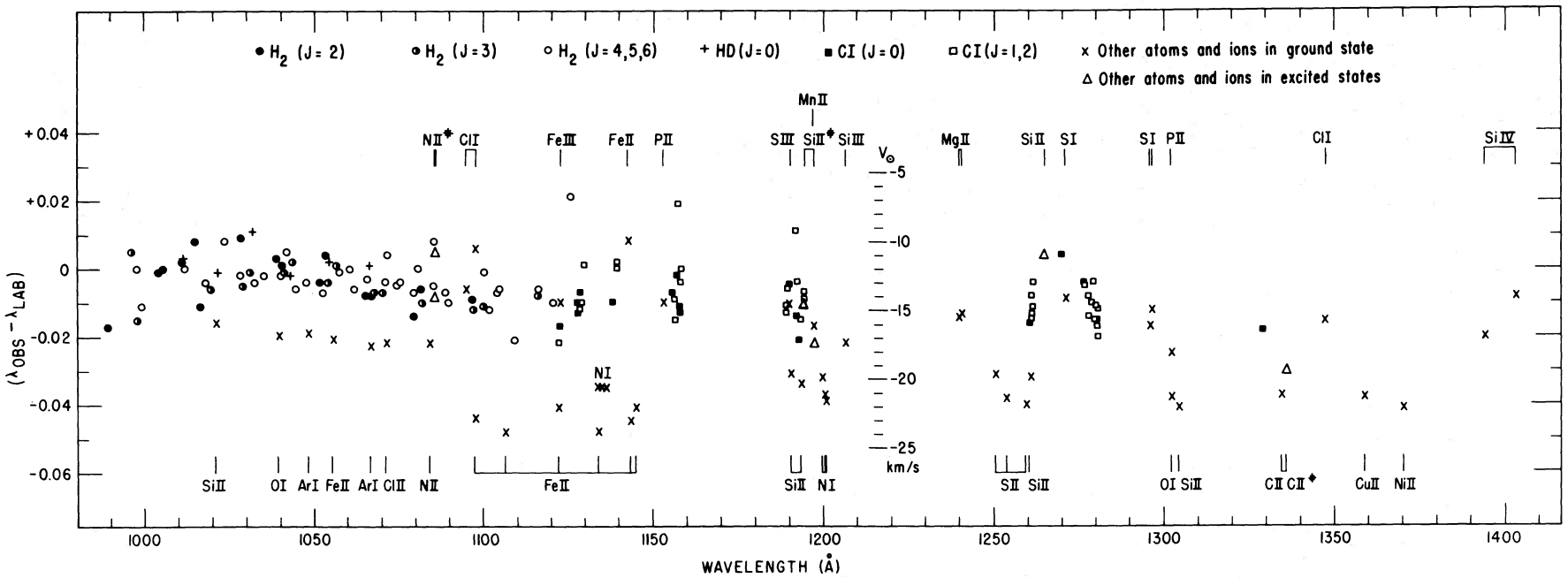


FIG. 3.—Deviations of interstellar line centers in ζ Oph from laboratory wavelengths for the continuous U1 scan. The observed wavelengths were obtained from the standard *Copernicus* scale. The heliocentric velocity scale at Lα was based on the assumption that the Lα airglow emission was at rest relative to the center of the Earth. This scale is not applicable at other wavelengths.

line seen in figure 2*b* at the bottom of the interstellar absorption line has provided an absolute calibration at this wavelength. It was assumed that the main contribution to this emission was at rest relative to the Earth, consistent with the observations of Morton and Purcell (1962). A scale of heliocentric velocities $V_\odot$ corresponding to $\lambda_{obs} - \lambda_{lab}$ has been included at L$\alpha$ in figure 3. If the reader wishes to compare $\zeta$ Oph with scans of other *Copernicus* stars reduced with the same wavelength scale, the observed wavelengths in tables 1 and 2 were calculated relative to a star with an assumed heliocentric radial velocity of $-19.0$ km s$^{-1}$.

The $H_2$ lines have been plotted using three types of circles since Spitzer and Cochran (1973) found that the rotational levels $J'' = 0$, 1, 2, and 3 in the lowest vibrational level are populated with a mean Boltzmann excitation temperature of 94° K while the higher levels $J'' = 3$, 4, 5, and 6 are best represented with a temperature of 327° K. Unfortunately the wide $R(0)$ and $R(1)$ lines are blended, and the $P(1)$ also are rather wide, so that velocity data were available only for $J'' \geq 2$. Nonetheless, the figure shows that there is no systematic velocity separation of the remaining rotational levels within 0.005 Å or 1.4 km s$^{-1}$. The two population distributions appear to occur within the same cloud, consistent with the single curve of growth having $b = 3.8$ km s$^{-1}$, which Spitzer and Cochran (1973) found for the $H_2$ lines in $\zeta$ Oph. The lack of separation among the lines originating from various levels appears contrary to the velocity differences that would be expected if the high-temperature component were heated by interstellar shocks as proposed by Aannestad and Field (1973). The coincidence of $H_2$ and HD velocities shows that both molecules probably originate in the same region, as expected from the theoretical considerations of Black and Dalgarno (1973*a*).

The pattern of the $H_2$ lines is continued to longer wavelengths by neutral atoms such as C I including its excited levels, S I, and Cl I, along with Mg II and possibly P II and Mn II. The absolute scale at L$\alpha$ suggests that the C I lines originate mainly in the cloud at $-14.4$ km s$^{-1}$, where Hobbs (1973*a*) found K I and the strongest component of Na I. The $H_2$, HD, S I, and Cl I probably have the same velocity, though it is not possible with the ultraviolet data to decide with certainty whether there is a separation between the molecules and atoms corresponding to the 1.8 km s$^{-1}$ that Hobbs (1973*a*) found between $CH^+$ and K I. However, since the CO radio emission is at $-14.1$ km s$^{-1}$, the $H_2$ very likely has the same heliocentric velocity, which the K I line gave as $-14.4$ km s$^{-1}$.

The neutrals N I, O I, and Ar I and ions such as C II, Si II, S II, Cl II, and Fe II show a distinct separation from the $H_2$ and C I with radial velocities about 5 km s$^{-1}$ more negative. The simplest interpretation is that the interstellar medium in this direction consists of at least two major clouds, with a definite separation of species. It is possible for C II and S II to be concentrated in a different cloud from the C I and S I, but it is difficult to understand why Mg II, P II, and Mn II would not have the same velocity as the other ions. However, when we note that the atomic lines forming the upper group of points in figure 3 are all relatively weak while the lower group consists mainly of saturated lines, the following picture seems likely. The weak lines originate primarily in the densest cloud,

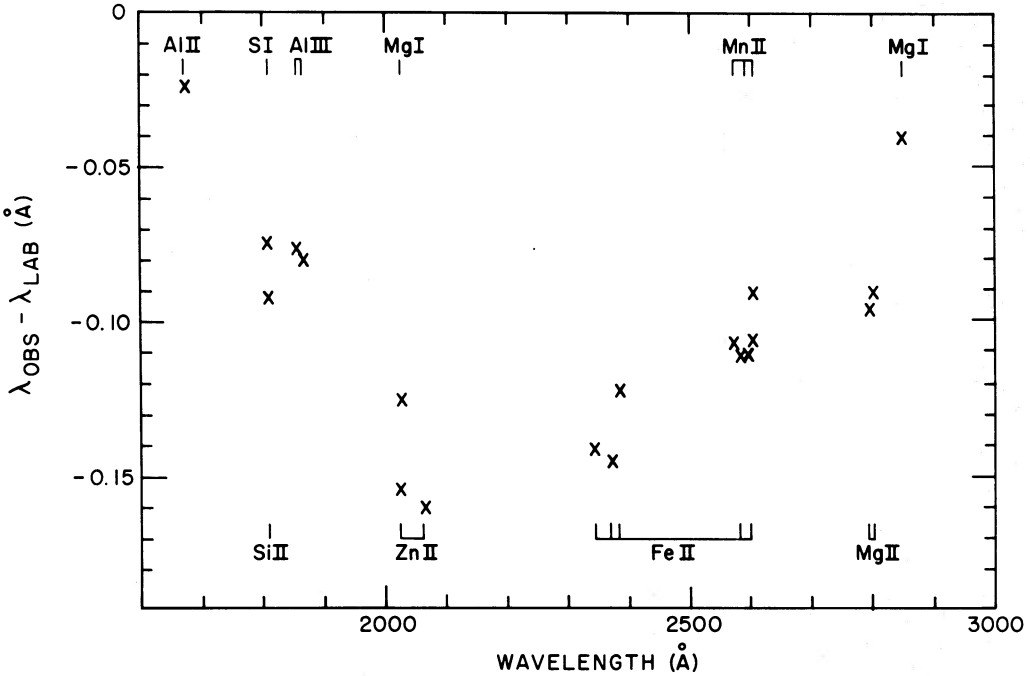


FIG. 4.—Deviations of interstellar line centers in $\zeta$ Oph from laboratory wavelengths for the V1 scans

which can be identified with the strong visible lines at $-14.4$ km s$^{-1}$. A cloud at this velocity or at $-12.6$ km s$^{-1}$, where the 21-cm emission is greatest, is presumed to have the majority of the C II, N I, O I, Si II, S II, Ar I, and Fe II. These lines lie well up on the saturated Doppler region of the curve of growth where a large change in column density has little effect on an equivalent width. Thus the lines of these abundant ions occurring in a lower-density cloud, such as the one at $-25.5$ or $-27.6$ km s$^{-1}$ seen in the visible, could contribute nearly half the observed equivalent width even if most of the column density is in the cloud at $-12.6$ or $-14.4$ km s$^{-1}$. Since the instrumental resolution ranges between 15 km s$^{-1}$ at 1000 Å and 11 km s$^{-1}$ at 1400 Å, the strong lines would not be separated, and their centers would be between 5 and 8 km s$^{-1}$ from the weak lines. There is some evidence for this picture from lines of intermediate strength such as λ1152.81 of P II which is definitely asymmetric with a weaker component about $-15$ km s$^{-1}$ from the center of the deepest part. Since the centers of the stronger $H_2$ lines are not shifted relative to the weaker ones, there seems to be little or no $H_2$ in the $-28$ km s$^{-1}$ cloud. On the other hand, λ1302 of O I, which is the strongest interstellar line after H I and $H_2$, shows evidence for an additional component on the long-wavelength edge.

The plot of the wavelength corrections for the V1 lines in figure 4 shows that the errors in some parts of this scale must be rather large. Nevertheless, the lines of Mg II, Mn II, Fe II, and Zn II appear to follow a pattern that lies about $-4$ or $-5$ km s$^{-1}$ from the two lines of Mg I, and Si II lies about $-3$ km s$^{-1}$ from S I. In contrast with figure 3, when the lines of Mg II and Mn II are sufficiently strong they also can be separated in velocity from the neutrals. However, since the relatively strong lines of C I λ1328.8 and Mg I λ2852.1 do not seem to be shifted significantly relative to the weaker neutrals, C I and Mg I must be more concentrated in the $-14.4$ km s$^{-1}$ cloud than the first ions.

### *b) Separations Expected from Ionization Equilibrium*

The separation of species into different clouds is consistent with what might be expected from the ionization potentials (see table 7, where values are quoted from Moore 1970*b*). Since any concentration of neutral hydrogen will absorb all stellar photons more energetic than the Lyman limit at 13.598 eV, the ions requiring higher energies will exist only in regions where the hydrogen is ionized, while any ion such as C I with a lower potential mainly will be transformed to the next highest state. The low abundances of even higher ion states toward the unreddened stars discussed by Rogerson, York *et al.* (1973), and the low density of hydrogen ions required at the centers of clouds by Jura (1974*b*) to explain the observed $H_2$ and HD, imply that neither X-rays nor cosmic rays contribute much to the ionization equilibrium.

Therefore, within the H I clouds, N, O, and Ar should be neutral, but Li, C, Na, Mg, Al, Si, P, S, Cl, K, Mn, Fe, Ni, Cu, and Zn ought to be mainly singly ionized unless there is a region where the electron density $n_e$ is exceptionally high. Similarly Ca and Ti are expected to be doubly ionized, but the ionization and recombination coefficients tend to favor Ca II, and Wallerstein and Goldsmith (1974) have argued that there are insufficient photons shortward of 913.0 Å to produce much Ti III in an H I cloud. Thus it is reasonable for N I, O I, Ar I, C II, Mg II, Si II, S II, Cl II, Mn II, Fe II, Ni II, Cu II, and Zn II in figures 3 and 4 to show evidence of significant abundances in at least two clouds, while the C I, Mg I, S I, and Cl I are mainly in a single cloud with high $n_e$. Consequently it will be assumed that these last four neutrals originate in the $-14.4$ km s$^{-1}$ cloud where the visible lines of Li I, Na I, K I, Ca I, and Fe I also are strongest. It would not be surprising to have $H_2$, HD, and CO also concentrated in this cloud, where the volume density of all particles must be highest. The $CH^+$ appears to occur entirely at $-12.6$ km s$^{-1}$ where the 21-cm emission is peaked. The velocity data on Al II and P II are inconclusive, but these ions very likely are distributed like Mg II and Fe II. The agreement between the velocities of the C I and the weak Mg II and Mn II lines in figure 3 implies that most of these ions are at $-14.4$ or $-12.6$ km s$^{-1}$, with less than 20 percent in clouds around $-28$ km s$^{-1}$; otherwise the effect of the second component would be noticeable.

Since N II, N III, Al III, Si III, Si IV, S III, and Fe III require ionizing wavelengths short of the Lyman limit, these ions are expected to be located only in the Strömgren sphere around ζ Oph or between the H I clouds, where Torres-Peimbert, Lazcano-Araujo, and Peimbert (1974) have argued that the hydrogen must be ionized by the radiation from the significant fraction of hot stars which have no surrounding Hα emission. O I has a slightly larger ionization potential than H I, with the result that O II will be found only in H II regions, and the majority of the O I should be with the H I. The positions for N II, Si III, S III, and Fe III in figure 3 and Al III in figure 4 are consistent with the hypothesis that these lines originate both in the Strömgren sphere at $-8$ km s$^{-1}$ and between the H I clouds along the rest of the line of sight to ζ Oph.

The excited fine-structure lines of C I* and C I** have the same velocities as C I, and the C II* line is similar to C II. The N II** line must originate in the H II regions, and evidence will be given later that Si II* also comes mainly from the same regions.

### *c) Summary of Velocity Assignments*

The major contributions to the column density of each ion and molecule appear to have the following heliocentric velocities:

H II Regions:

$-8.0$ km s$^{-1}$, Strömgren sphere and other intercloud regions at more negative velocities: H II, N II, N II**, Al III, Si II*, Si III, Si IV, S III, Fe III.

H I Clouds:
- $-9.0$ km s$^{-1}$; some Na I, Ca II.
- $-12.6$ km s$^{-1}$; some H I, Ca II; all $CH^+$, $^{13}CH^+$, and some Na I.
- $-12.6$ or $-14.4$ km s$^{-1}$; most C II, C II*, N I, O I, Mg II, Al II, Si II, P II, S II, Cl II, Ar I, Mn II, Fe II, Ni II, Cu II, and Zn II.
- $-14.4$ km s$^{-1}$; some H I, Ca II, all $H_2$, HD, and most CO, CH, CN, CN*, Li I, C I, C I*, C I**, Na I, Mg I, S I, Cl I, K I, Ca I, and Fe I.
- $-17.5$ km s$^{-1}$; some Na I, Ca II.
- $-25.5$ km s$^{-1}$; some Na I and possibly some Ti II.
- $-25.5$ or $-27.6$ km s$^{-1}$; up to 20% of the neutrals and first ions also present at $-12.6$ or $-14.4$ km s$^{-1}$.
- $-27.6$ km s$^{-1}$; Ti II and some Na I, Ca II.

Of course, the ultraviolet lines may be formed in additional clouds which are not seen in the visible. Many of the neutrals associated with the $-14.4$ km s$^{-1}$ cloud are likely to be present in all the clouds where Na I has been detected, and the first ions along with N I, O I, and Ar I may be found in all the H I clouds to some extent. Some first ions also are possible in the H II regions. However, the curve-of-growth analyses in the next section will show that the velocity distributions of C I, Na I, S I, and Mg I are very different from those of N I, Mg II, Si II, S II, Ar I, and Fe II. The electron densities derived in § V imply that C I, Mg I, S I, and Ca I can be represented by one distribution, and C II, Mg II, S II, and Ca II by another.

## IV. VELOCITY DISPERSIONS AND COLUMN DENSITIES

### *a) Atoms and Ions Other than Hydrogen*

In order to obtain column densities for many of the species listed in table 1, it is necessary to determine the velocity profile for each kind of absorbing particle. The simplest procedure is to assume that each absorption line is formed in a region with a Maxwellian distribution of particle velocities represented by the Doppler width $b$, where $b/2^{1/2}$ is the velocity dispersion of the absorbers in the line of sight. The resulting line profile is the usual Voigt function. This assumption is not consistent with the evidence discussed in the previous section that the strong lines originate in at least two separate clouds. It is possible to obtain some information about the distribution of velocities from the interferometer scans of visible lines, as shown by Hobbs (1973*a*) or Jenkins (1973). Near the saturated portion of a profile, the correction for parasitic light becomes very important but an additional constraint is available from the equivalent widths of the weak Na I lines at 3303 Å. However, then it is necessary to assume that all ions have the same distribution, which certainly is not true for Ti II which appears in only the $-28$ km s$^{-1}$ clouds toward $\zeta$ Oph. For a group of 10 stars, Hobbs (1974) has inferred that the K I column density varies as the square of the H I column density, implying that K I and hence Li I, C I, Na I, etc., lie mainly in the densest cloud where the ionization equilibrium favors the neutrals. Fortunately there are many cases where the derived column density is not affected seriously by the assumed velocity distribution because either the ion has a line weak enough to escape significant saturation, or it has a strong line near the damping part of the curve of growth.

Nevertheless, there are a number of lines which appear to be on the saturated Doppler region of the curve of growth where small uncertainties in the velocity distribution produce large differences in the derived column density. In the analysis of $\zeta$ Oph, it was possible to take advantage of the multiple lines available from each of several ions and construct an empirical curve of growth. Since figure 3 indicates similar mean radial velocities for C II, N I, O I, Si II, S II, Cl II, Ar I, Fe II, Ni II, and Cu II, it was reasonable to assume that these species are distributed over the absorbing clouds with the same relative abundances. Figure 4 showed that Mg II, Mn II, and Zn II should be similar to Fe II, and Al II and P II were added to the list because they should follow the same ionization pattern. Since N I, Mg II, Si II, S II, Ar I, and Fe II each has two or more lines with $f$-values differing by more than a factor 2, these species were used to define the empirical curve of growth given by the points in figure 5. The group of points for each atom or ion was shifted horizontally until a smooth curve was defined.

The figure shows that the run of points can be approximated rather well by a simple curve of growth corresponding to a single cloud with $b = 6.5 \pm 0.5$ km s$^{-1}$. This relatively large value should be interpreted as some combination of internal velocities in each cloud and the relative velocities of these clouds. The only inconsistency seems to be that damping in $\lambda\lambda$1190, 1193 of Si II ought to make these points higher than observed. Comparison of the equivalent widths of the weak lines of Si II* show that the $f$-values for the $\lambda$1194 multiplet may be too large relative to the $\lambda$1263 multiplet by a factor 2. However, the absence of $\lambda$1308 of Si II* suggests the error is with $\lambda$1263, for which Curtis and Smith (1974) had a large cascading correction in their lifetime measurement. If $f(\lambda 1194)$ is correct, figure 5 implies that either $f(\lambda 1808)$ or $W_\lambda(\lambda 1808)$ must be wrong. A similar empirical curve of growth has been derived by de Boer (1974). He used Hobbs's (1973*a*) profiles along with the equivalent widths of the Na I near-ultraviolet lines to obtain the relative velocities of the clouds and their internal $b$ values. Then, from the equivalent widths of the Fe II lines, he was able to find a model for the amount of this ion in each cloud, and hence the complete Fe II curve of growth.

Since absolute $f$-values were available, the curve in figure 5 determined densities of the plotted ions, and any other ion which could be assumed to have the same velocity distribution over the clouds if $f$ and $W_\lambda$ are known. However, to show the uncertainties still possible in the curve of growth, the column densities in table 7 were quoted for the simple curve of growth with $b = 7.0$ and 6.0 km s$^{-1}$. For Mg II and Fe II the data implied slightly tighter ranges on $b$, whereas, with weaker lines like Cl II and Cu II and the upper

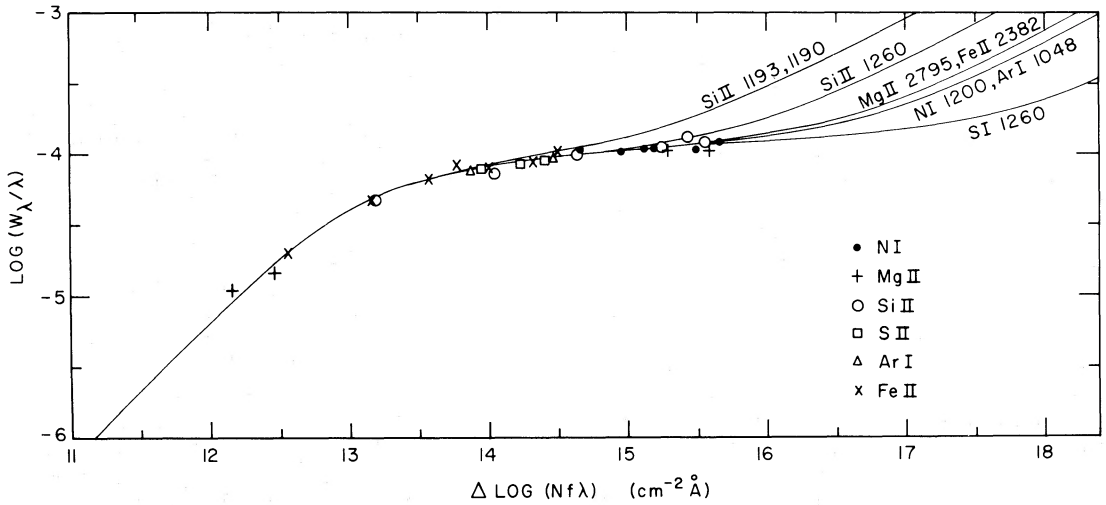


FIG. 5.—Empirical curve of growth for the dominant ion states expected in H I clouds. The solid lines were drawn for a Maxwellian velocity distribution with $b = 6.5$ km s$^{-1}$ and the damping constants appropriate for the lines labeled in the upper right corner. The horizontal scale was labeled to give log $N$(cm$^{-2}$) for Fe II λ2382.

limits on several ions, a $b$ as low as 0.7 km s$^{-1}$ was considered because the empirical curve of growth was not defined below Mg II λ1240.395. The spread in Si II densities allowed for the possible errors in $f$ values. The two lines of P II required an unusually large $b \sim 12$ km s$^{-1}$. It is more likely that one of the $f$-values is in error, so log $N$ was derived from the weaker line which was assumed to have the more

TABLE 7

ATOMIC COLUMN DENSITIES TOWARD ζ OPHIUCHI

| Ion | I.P. (eV) | $b$ (km s$^{-1}$) | log $N$ (cm$^{-2}$) | Ion | I.P. (eV) | $b$ (km s$^{-1}$) | log $N$ (cm$^{-2}$) |
|---|---|---|---|---|---|---|---|
| H I | 13.598 | damped | 20.72 | S I | 10.360 | fig. 6 | 13.93 |
| H I + $2H_2$ | ... | ... | 21.13 | S II | 23.33 | 7.0–6.0 | 15.86–16.24 |
| Li I | 5.392 | ≥0.7 | 9.36 | S III | 34.83 | 7.5–5.5 | 14.70–15.00 |
| Be II | 18.211 | ≥0.7 | < 10.96 | Cl I | 12.967 | fig. 5 | 14.03 |
| B II | 25.154 | ≥0.7 | < 11.00 | Cl II | 23.81 | 7.0–6.0 | 13.08–13.63 |
| C I | 11.260 | fig. 6 | 15.35 ± 0.15 | Cl III | 39.61 | ≥1.8 | < 14.75 |
| C I* | 11.258 | fig. 6 | 15.05 ± 0.07 | Ar I | 15.759 | 7.0–6.0 | 14.90–15.22 |
| C I** | 11.255 | fig. 6 | 14.40 ± 0.07 | K I | 4.341 | fig. 6 | 11.90–12.39 |
| C I total | 11.260 | fig. 6 | 15.56 ± 0.17 | Ca I(−14) | 6.113 | ≥0.7 | 9.72 |
| C II | 24.383 | 7.0–6.0 | 16.80–17.15 | Ca I(−28) | 6.113 | ≥0.5 | < 9.11 |
| C II* | 24.375 | 7.0–6.0 | 14.86–15.12 | Ca II(−14) | 11.871 | 7.0–1.8 | 11.64–11.73 |
| C IV | 64.492 | ≥3.1 | < 12.67 | Ca II(−28) | 11.871 | 2.3–0.5 | 11.05–11.14 |
| N I | 14.534 | 7.0–6.0 | 16.22–16.70 | Ca II total | 11.871 | | 11.74–11.83 |
| N II | 29.601 | 13.0–5.5 | 14.50–16.86 | Ti I | 6.82 | ≥0.5 | < 11.25 |
| N II* | 29.595 | 13.0–2.9 | 13.43–17.04 | Ti II(−14) | 13.58 | ≥0.7 | < 11.00 |
| N II** | 29.585 | 13.0–2.9 | 13.83–14.23 | Ti II(−28) | 13.58 | 2.3–0.5 | 11.42–11.54 |
| N III | 47.448 | ≥5.5 | < 13.94 | Ti III | 27.491 | ≥1.6 | < 12.39 |
| N V | 97.888 | ≥2.9 | < 12.29 | V I | 6.74 | ≥0.7 | < 11.05 |
| O I | 13.618 | 7.0–6.0 | 17.28–17.47 | V II | 14.65 | ≥0.7 | < 12.61 |
| O I* | 13.598 | ≥0.7 | < 12.88 | V III | 29.310 | ≥1.5 | < 12.44 |
| O VI | 138.116 | ≥2.7 | < 13.38 | Cr I | 6.766 | ≥0.7 | < 11.06 |
| Na I(−14) | 5.139 | fig. 6 | 13.86 ± 0.1 | Cr II | 16.50 | ≥0.7 | < 12.35 |
| Na I(−28) | 5.139 | 0.48 | 11.68 | Cr III | 30.96 | ≥1.5 | < 13.28 |
| Mg I | 7.646 | fig. 6 | 14.15 | Mn I | 7.435 | ≥0.7 | < 11.58 |
| Mg II | 15.035 | 6.5–5.8 | 14.91–15.27 | Mn II | 15.640 | 7.0–6.0 | 13.26–13.33 |
| Al I | 5.986 | ≥0.7 | < 10.21 | Fe I | 7.870 | ≥0.7 | 11.52 |
| Al II | 18.828 | 6.5 | 12.09–12.41 | Fe II | 16.18 | 7.0–6.5 | 14.48–14.64 |
| Al III | 28.447 | 14.0–5.5 | 12.63–12.72 | Fe II* | 16.13 | ≥0.7 | < 12.2 |
| Si I | 8.151 | ≥0.7 | ≤12.58 | Fe III | 30.651 | 10.0–5.5 | 13.57–13.62 |
| Si II | 16.345 | 7.0–6.0 | 14.80–15.30 | Co I | 7.86 | ≥0.7 | < 13.23 |
| Si II* | 16.309 | 13.0–2.0 | 11.86–12.50 | Co II | 17.06 | ≥0.7 | < 14.36 |
| Si III | 33.492 | 13.0–5.5 | 13.13–14.72 | Ni I | 7.635 | ≥0.7 | < 12.24 |
| Si IV | 45.141 | 8.0–2.0 | 12.57–12.84 | Ni II | 18.168 | 7.0–6.0 | 12.96–13.27 |
| P II | 19.725 | 6.5 | 13.37–13.56 | Cu I | 7.726 | ≥0.7 | < 10.93 |
| P III | 30.18 | ≥1.9 | < 13.06 | Cu II | 20.292 | 7.0–6.0 | 11.79–12.08 |
| P V | 65.023 | ≥1.9 | < 11.82 | Zn II | 17.964 | 7.0–6.0 | 13.23–13.32 |

reliable transition probability. The range in column density for this line and for Al II, Ni II, and Cu II was extended to include the 2 $\sigma$ uncertainty in $W_\lambda$.

As discussed below, there is evidence from the visible lines for the presence of one high-density cloud with $b = 0.7$ to 0.9 km s$^{-1}$. In order to test whether such a cloud could explain the ultraviolet lines, theoretical Voigt profiles were computed as described by Morton and Morton (1972) for comparison with the strongest line of each ion assuming a Maxwellian velocity distribution with a single $b$ and a Gaussian instrumental profile with 0.05 or 0.1 Å FWHM. The observed profiles required $b \geq 5.5$ km s$^{-1}$ for C II, N I, O I, Mg II, Si II, Ar I, and Fe II and $b \geq 4.0$ km s$^{-1}$ for S II, primarily as a consequence of the absence of significant damping wings. In the case of O I, there is an indisputable upper limit on the curve of growth for pure damping, where $\log N = 17.73$ for $b \leq 2$ km s$^{-1}$. Any larger Doppler width, due to either velocities within each cloud or to relative cloud motions, would only decrease $\log N$. The presence of the O I intersystem line at $\lambda$1355.6 is rather questionable. The lower limit $W_\lambda - 2\sigma$ implies that $\log N \geq 17.98$ for a pure Doppler curve of growth indicating that either the measurement is spurious or that Garstang's (1961) calculated $f$-value is too small by a factor of at least 1.8.

Higher ion stages which probably originate in H II regions would not be expected to have the same curve of growth as the H I material. However, profile fitting with a single Maxwellian component showed that $b \geq 5.5$ km s$^{-1}$ for the strong lines of N II and Si III, in order to obtain the observed width and avoid excessive damping wings. Such a lower limit on $b$ is reasonable for H II regions and is consistent with turbulent velocities corresponding to $b$ between 27.5 and 5.9 km s$^{-1}$ obtained by Mezger and Höglund (1967) from profiles of the H 109$\alpha$ recombination line. Pedlar and Matthews (1973) required $b = 9.2$ and 9.3 km s$^{-1}$ to account for turbulence in the 166$\alpha$ line from the Rosette and North America H II regions, respectively. Therefore, in table 7, the strong lines of N II, Si III, S III, and Fe III were analyzed with $b$ ranging between 5.5 km s$^{-1}$ and an upper limit given by additional fitting with single-cloud profiles. In the case of the weaker lines, and the undetected ones which could be attributed to H II regions, $b$ was permitted to go as low as the value for a kinetic temperature of 7000°, ranging from 3.1 km s$^{-1}$ for carbon to 1.4 km s$^{-1}$ for iron. The N II** lines appear to fit a simple curve of growth with $4.5 \geq b \geq 3.0$, after taking account of the two transitions labeled as $\lambda$1085.545. In table 7, a larger range was permitted because it had little effect on the derived $\log N$.

An empirical curve of growth was constructed in figure 6 for the neutral atoms which are likely to have similar velocity distributions according to the discussion in § III because their ionization potentials are less than 13.5 eV. The four Na I lines, which have the best determined equivalent widths and $f$-values, lie almost on a straight line which cannot be approximated with a single Maxwellian cloud velocity. Note that only the four components of the D lines near $-14$ km s$^{-1}$ were used here. Adding the absorption around $-28$ km s$^{-1}$ would have changed each $\log (W_\lambda/\lambda)$ by $+0.04$. It is clear that the analysis of the doublet ratio of the strongly saturated D lines in terms of one cloud would be seriously in error, as described by Nachman and Hobbs (1973) and de Boer and Pottasch (1974). However, the weaker lines were close enough to being unsaturated that they were fitted with the simple curve of growth for $b = 0.9$ km s$^{-1}$ giving the extrapolation

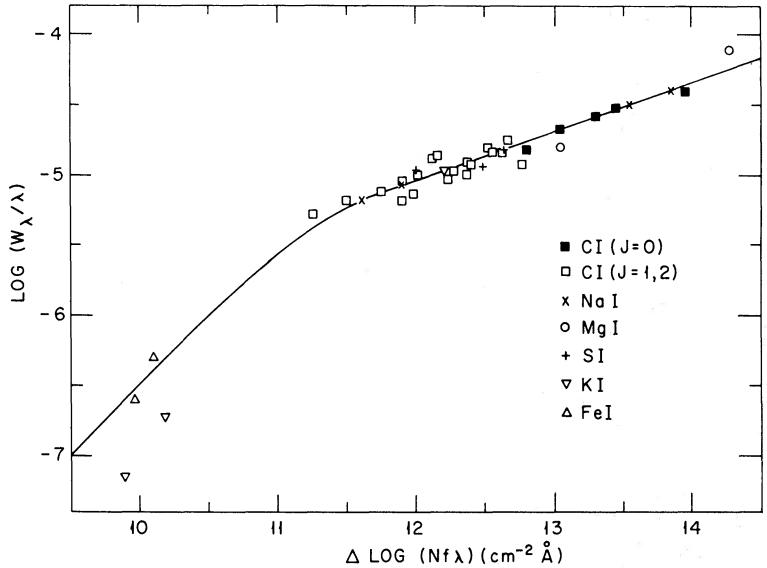


FIG. 6.—Empirical curve of growth for neutral atoms that can be ionized easily in H I regions. The solid line was based on the Na I points, with the weaker pair fitted to a Maxwellian curve with $b = 0.9$ km s$^{-1}$ for the smallest equivalent widths. The stronger pair refer to only the four clouds near $-14$ km s$^{-1}$ because the lines of C I appear to have no significant contribution from the clouds at $-28$ km s$^{-1}$. The horizontal scale was labeled to give $\log N$(cm$^{-2}$) for Na I $\lambda$5890.

to lower values of log $Nf\lambda$ in the figure. In this way the empirical curve was related to an absolute scale of column densities so that log $N$(Na I) = 13.86. If a single-cloud model had been adopted for the D lines, it would have given $b = 4.2$ and log $N = 12.59$, while all four lines would have given a poor fit with $b = 2.5$ and log $N = 13.53$. The unsaturated limit for the weakest line implies log $N = 13.54$, and the lower limit of $b = 0.7$ described below gives log $N = 14.08$. These limits seem unnecessarily wide; the true value probably lies within ±0.1 of 13.86.

The interval in the empirical curve of figure 3 between the Na I doublets can be filled in with the numerous lines of C I, as described by de Boer and Morton (1975). They adopted $f(\lambda 1260.736) = 0.038$ from a beam-foil lifetime and derived all other oscillator strengths from unsaturated lines in ζ Pup and $\gamma^2$ Vel along with comparisons of ζ Oph lines within the same multiplet. There was considerable scatter in the C I points, but they showed that the straight line in figure 6 is an acceptable approximation. The three single lines of S I also fit, and the two lines of Mg I make a reasonable extrapolation. Thus column densities were obtained for these atoms and for the one unblended line of Cl I. The agreement among the curves for Na I, C I, and S I supports the assumption that all such ions have similar velocity distributions. The velocities implied by figures 3 and 4 for C I, Mg I, S I, and Cl I are consistent with neglecting the components of the D lines near −28 km s$^{-1}$. Including them would have reduced the abundances of Mg I and ground-state C I by at most 0.15 dex.

It had been hoped that the three K I lines, which cover a wide range in $f$, would define the left-hand part of the curve of growth in figure 6, but an inconsistency soon became evident. Hobbs's (1973*a*) scan of λ7699 showed a single cloud at −14.4 km s$^{-1}$ with a velocity profile of 1.7 km s$^{-1}$ FWHM which corresponds to $b = 0.72$ km s$^{-1}$ after correction for an instrumental profile of 1.2 km s$^{-1}$ FWHM. The actual $b$ even could be a little smaller since this K I line consists of two hyperfine components separated by 0.36 km s$^{-1}$ (Kusch and Taub 1949). Unfortunately, when this line was fitted to a simple Maxwellian curve of growth with the weak pair of K I lines observed by Shulman *et al.* (1974), it was found that $b = 1.8$ (+1.1, −0.5) km s$^{-1}$. Since the equivalent widths of the weak lines are not likely to have been underestimated by a large factor, and the mean error for three measurements of λ7699 is only 10 percent of $W_\lambda$, the discrepancy in $b$ values must be due to an overestimate of the interferometer width or too small a ratio of $f(7699)/f(4047)$ by about a factor 10. The strong line required log $N$(K I) = 13.17 with $b = 0.7$ for a single cloud and 12.39 from the empirical curve of growth, while the weak pair gave 11.90 almost independently of $b$. The range 11.90 to 12.39 has been adopted for table 7. Hobbs (1973*a*) found log $N$ = 11.81 by integrating the optical depth over the profile without correcting for the instrumental width, whereas his equivalent width $W_\lambda = 76$ mÅ and $b = 0.7$ km s$^{-1}$ imply log $N = 12.90$, indicating that the instrumental broadening should not have been ignored if the line really is so narrow. Since a single dense cloud with $b$ as small as 0.7 km s$^{-1}$ may be present as the main source of the weakest lines, all neutrals and first ions with $W_\lambda/\lambda$ below the lowest Na I point on the empirical curve of growth in figure 6 were analyzed with $b = 0.7$ unless they belonged to the clouds near −28 km s$^{-1}$.

The severe depletion of calcium may have left this element with a unique velocity distribution over the clouds so that it is not surprising that the H and K lines around −14 km s$^{-1}$ do not fit the Na I curve of growth. Since the lines are nearly unsaturated, the doublet ratio was used with the result that $b = 1.8$ and log $N = 11.73$, compared with 11.71 which Hobbs (1973*a*) obtained by integrating over the K profile, and 11.64 if $b = 7.0$ km s$^{-1}$. The source of the weak lines of Si II* is uncertain so that $b$ values appropriate for both the first ions and H II regions were considered and some allowance was made for uncertainties in the $f$-values. The ratio Si II*/Si II probably lies within a factor 2 of $10^{-3}$.

In the cloud near −28 km s$^{-1}$, all of the lines are weak. The ratio of the D lines implied $b = 0.5$, while the observed widths of both Na I and Ca II corresponded to $b \leq 2.3$ km s$^{-1}$. Consequently these limits were adopted for the analysis using the simple curve of growth. For the comparison of Ca II with other first ions, it might have been more appropriate to use the total equivalent widths of 26.0 and 44.5 mÅ, for which $b = 3.0$ and log $N = 11.79$.

### *b) Hydrogen Atoms and Molecules*

Fortunately the interstellar Lα line is so strong that it lies well up on the damping part of the curve of growth where any possible $b$ has no effect. However, the wide damping wings and the uncertainty of the true level of the continuum prevented a reliable direct measurement of $W_\lambda$. Instead, the observed intensity was corrected for the scattered light and then multiplied by exp $(+\tau_\lambda)$ for a range of column densities and corresponding optical depths $\tau_\lambda$ at wavelength $\lambda$ in a Lorentz profile until the best representation was obtained for the stellar spectrum in the Lα wings. This procedure gave $N$(H I) = (5.2 ± 0.2) × $10^{20}$ cm$^{-2}$. From rocket spectra, Smith and Stecher (1971) obtained (4.6 ± 1.5) × $10^{20}$ cm$^{-2}$ while Morton *et al.* (1972) reported (5 ± 2) × $10^{20}$ cm$^{-2}$. Grayzeck and Kerr (1974) found that the 21-cm emission corresponds to 1.3 × $10^{21}$ cm$^{-2}$, indicating that considerable H I beyond ζ Oph must contribute to the radio profile. According to Spitzer, Drake *et al.* (1973) and Spitzer *et al.* (1974), the total column density in all levels of $H_2$ is 4.2 × $10^{20}$ molecules cm$^{-2}$ so that the total for H particles excluding H II is $N_H$ = 1.36 × $10^{21}$ cm$^{-2}$. Considerable ionized hydrogen could be present between the neutral clouds, as proposed by Torres-Peimbert *et al.* (1974), as well as in the Strömgren sphere around ζ Oph (see § V).

Two of the HD lines in table 5 are rather weak for their $f$-values, but all six lines fit a curve of growth with $b = 3.8$ km s$^{-1}$ if $W_\lambda$ for (5,0) is too large by 2 σ

and the $W_\lambda$'s for (7,0) and (8,0) are too small by 2.6 $\sigma$ and 1.7 $\sigma$, respectively. Then $N(\mathrm{HD}) = 1.6 \times 10^{14}$ cm$^{-2}$, the same value that Spitzer *et al.* (1974) determined from the (3,0) and (4,0) lines. The upper limit on HD in the lowest excited rotational level also was based on $b = 3.8$ km s$^{-1}$ obtained from the $H_2$ lines.

### c) *Other Molecules*

When the equivalent widths and *f*-values of the CO lines were summed over all rotational transitions, the curve of growth showed saturation in the stronger lines, so that their analysis will have to wait for detailed calculations depending on both the velocity distribution and the rotational temperature. However, the two weakest lines lie close to the linear curve, indicating that either $b$ or $T_{\mathrm{rot}}$ may be large enough that saturation corrections can be ignored. Then $1.1 \times 10^{15} \leq N(\mathrm{CO}) \leq 1.6 \times 10^{15}$ cm$^{-2}$ if $b \geq 3.0$ km s$^{-1}$, which is a reasonable lower limit if CO and $H_2$ are in the same clouds. Alternatively, the CO points approximately fit the curve of growth for the neutrals in figure 6, as might be expected for a molecule in the densest cloud. Then the weak lines, which appear to have only $R(0)$ components, give $N(\mathrm{CO}) = 5.6 \times 10^{15}$ cm$^{-2}$. For comparison, Jenkins *et al.* (1973) found $4.6 \times 10^{14}$ from lower-resolution *Copernicus* scans, while Smith and Stecher (1971) derived $7.6 \times 10^{15}$ cm$^{-2}$ from a rocket flight, with both papers adopting the smaller *f*-values noted in § III*c*. No lines of $^{13}C^{16}O$ were detected shortward of 1420 Å, giving the limit $N(^{13}C^{16}O) < 3.0 \times 10^{13}$ if $b \geq 3$ km s$^{-1}$, and $N < 5.6 \times 10^{13}$ if $b$ is as low as 0.7 km s$^{-1}$, the value derived from Hobbs's (1973*a*) profile of K I $\lambda$7699 after correction for an instrumental FWHM of 1.2 km s$^{-1}$. Smith and Stecher believed they had detected some of the stronger $^{13}C^{16}O$ lines longward of 1420 Å and concluded $N(^{13}C^{16}O) = 7.2 \times 10^{13}$, for a rather special assumption regarding the effective $b$. Additional scans for the $^{13}C^{16}O$ lines and a proper curve-of-growth analysis of the $^{12}C^{16}O$ lines are needed before this molecule can give as useful limit on $^{12}C/^{13}C$ as obtained from $CH^+$.

The *Copernicus* scans also provided upper limits on column densities for OH, HCl, $C_2$, $NO^+$, SiO, and $H_2O$, with $b \geq 0.7$ km s$^{-1}$. The limits for several of these molecules could change with improvements in

TABLE 8

MOLECULAR COLUMN DENSITIES TOWARD $\zeta$ OPHIUCHI

| Molecule | $v''$ | $J''$ | $b$ (km s$^{-1}$) | log $N$ (cm$^{-2}$) | R* |
|---|---|---|---|---|---|
| $H_2$ | 0 | 0 | 3.8 | 20.46 | 3 |
| | 0 | 1 | 3.8 | 20.10 | 3 |
| | 0 | 2 | 3.8 | 18.56 | 4 |
| | 0 | 3 | 3.8 | 17.07 | 4 |
| | 0 | 4 | 3.8 | 15.68 | 4 |
| | 0 | 5 | 3.8 | 14.77 | 4 |
| | 0 | 6 | 3.8 | 13.58 | 4 |
| | 1 | 0 | 3.8 | < 12.84 | 4 |
| | 1 | 1 | 3.8 | < 13.08 | 4 |
| | 1 | 2 | 3.8 | < 13.00 | 4 |
| | 2 | 0 | 3.8 | < 12.64 | 4 |
| | total | | 3.8 | 20.62 | 3,4 |
| HD | 0 | 0 | 3.8 | 14.20 | 5 |
| | 0 | 1 | 3.8 | < 13.82 | 5 |
| CH | 0 | $\frac{1}{2}$ | $\geq 0.7$ | 13.53 | 2 |
| $CH^+$ | 0 | 0 | 2.5 | 12.97 | 5 |
| $^{13}CH^+$ | 0 | 0 | $\geq 0.7$ | 11.12 | 5 |
| NH | 0 | 0 | $\geq 0.7$ | < 13.87 | 1 |
| $C_2$ | 0 | 0 | $\geq 0.7$ | < 12.72† | 5 |
| CN | 0 | $\frac{1}{2}$ | $\geq 0.7$ | 12.68 | 1 |
| | 0 | $\frac{1}{2}, \frac{3}{2}$ | $\geq 0.7$ | 12.59 | 1 |
| OH | 0 | $\frac{3}{2}$ | $\geq 0.7$ | < 13.20† | 5 |
| | 0 | $\frac{3}{2}$ | $\geq 0.7$ | < 13.92 | 1 |
| CO | 0 | all | $\infty - 3.0$ | 15.03–15.20 | 5 |
| | | | fig. 6 | 15.75 | 5 |
| $^{13}C^{16}O$ | 0 | all | $\geq 0.7$ | < 13.75 | 5 |
| $CO^+$ | 0 | $\frac{1}{2}$ | $\geq 0.7$ | < 12.76 | 1,6 |
| $NO^+$ | 0 | 0 | $\geq 0.7$ | < 14.03 | 5 |
| MgH | 0 | $\frac{1}{2}$ | $\geq 0.7$ | < 12.63 | 1 |
| SiH | 0 | $\frac{1}{2}$ | $\geq 0.7$ | < 12.15 | 1,6 |
| SiO | 0 | 0 | $\geq 0.7$ | < 12.51† | 5 |
| HCl | 0 | 0 | $\geq 0.7$ | < 12.87† | 5 |
| $H_2O$ | 0 | | $\geq 0.7$ | < 12.38 | 5 |

* REFERENCES.—(1) Herbig 1968; (2) Black and Dalgarno 1973*b*; (3) Spitzer, Drake, *et al.* 1973; (4) Spitzer, Cochran, and Hirshfeld 1974; (5) this paper; (6) Bortolot and Thaddeus 1971.

† Limit on log $N$ was based on estimated *f*-value in table 5.

the rough estimates for the *f*-values. The significance of HCl is discussed at the end of § VI.

In addition, table 8 includes densities and upper limits derived from the visible and near-ultraviolet lines. Herbig (1968) found $b = 0.85$ km s$^{-1}$ for the $CH^+$ lines, while Smith, Liszt, and Lutz (1973) used improved ratios of *f*-values and concluded $b = 3.0$, closer to Hobbs's (1973*a*) value of $b = 2.5$ obtained from the profile of λ4232.5 and an instrumental FWHM of 1.0 km s$^{-1}$. Besides the uncertainty already noted for $W_\lambda$ of this line, the adopted *f*-values have included 0.0064 (Yoshimine *et al.* 1973), 0.012 (Frisch 1972), 0.017 (Black and Dalgarno 1973*b*), 0.02 (Smith, Liszt, and Lutz 1973), and 0.04 (Hobbs 1973*a*). For $f = 0.017$, $b = 2.5$ km s$^{-1}$, and $W_\lambda = 22.3$ mÅ, table 8 lists $N(CH^+) = 9.3 \times 10^{12}$ cm$^{-2}$. Similarly for $W_\lambda = 0.35$ mÅ, the column density of the isotopic molecule is $N(^{13}CH^+) = 1.3 \times 10^{11}$. Therefore $\alpha = {}^{12}C/{}^{13}C = 71$, close to $\alpha = 75$ deduced by Vanden Bout (1972) with $b = 2.2$ km s$^{-1}$.

For CH Herbig (1968), Frisch (1972), Black and Dalgarno (1973*b*) and Smith *et al.* (1973) obtained column densities between $3 \times 10^{13}$ and $5 \times 10^{13}$ cm$^{-2}$. The analysis of CN by Field and Hitchcock (1966) and Herbig (1968) showed that the population of the excited level of this molecule at 3.79 cm$^{-1}$ requires a rotational temperature near 3° K. Both CH and CN have weak enough lines that the densities are practically independent of *b* if $b \geq 0.7$ km s$^{-1}$.

## V. THE PROPERTIES OF THE STAR AND THE RADIATION FIELD

The further analysis of the data requires some knowledge of the physical parameters of ζ Oph in order to estimate the ionizing flux affecting both the H I and H II regions. According to Lesh (1968), $m_V = 2.56$, $B - V = +0.02$, and the MK type is O9.5 V. Since $(B - V)_0 = -0.30$ (Johnson 1966), $E_{B-V} = 0.32$ and $A_V = 3.0\, E_{B-V} = 0.96$. Comparison of the ratio of the equivalent widths of λ4471 of He I and λ4541 of He II observed by Conti and Alschuler (1971) with the theoretical results from the non–LTE unblanketed models of Auer and Mihalas (1972) gives $T_{\rm eff} = 34{,}000°$ K for $\log g = 4.0$. The surface flux of this model, obtained by interpolating the tabulations of Mihalas (1972), is $\pi F_\nu = 5.43 \times 10^{-3}$ ergs cm$^{-2}$ s$^{-1}$ Hz$^{-1}$ at $1/\lambda = 1.83\, \mu^{-1}$, and the value for the LTE model is almost the same. For comparison, the angular diameter of $(0.51 \pm 0.05) \times 10^{-3}$ arcsec measured by Hanbury Brown, Davis, and Allen (1974) combined with the flux at the Earth of $3.65 \times 10^{-20}$ ergs cm$^{-2}$ s$^{-1}$ Hz$^{-1}$ for $m_V = 0.0$ at $1/\lambda = 1.83\, \mu^{-1}$ reported by Oke and Schild (1970) gives $\pi F_\nu = 5.5 \times 10^{-3}$ ergs cm$^{-2}$ s$^{-1}$ Hz$^{-1}$. Lesh (1968) adopted $M_V = -4.9$ for O9.5 V and derived a distance of 200 pc. Therefore, the radius of the star is $R = 7.6 \times 10^{11}$ cm. According to Morton (1969), the bolometric correction is −3.20 for $T_{\rm eff} = 34{,}000°$ K and $M_{\rm Bol\odot} = 4.77$ so that $L/L_\odot = 1.4 \times 10^5$.

An Hα photograph of ζ Oph by Morgan, Strömgren, and Johnson (1955) showed an H II region $10° \times 7°$ centered on the star. A mean radius *r* of 4°.3 corresponding to 15 pc at 200 pc will be adopted for the following discussion. The usual theory for the Strömgren sphere, as described by Spitzer (1968), relates its radius *r* and the electron volume density $n_e$ according to

$$r^3 n_e^2 \alpha^{(2)} = 3R^2 N_L\,, \qquad (1)$$

where it is assumed the density is uniform and $n_e = n_{\rm H}$. Here the recombination coefficient to level 2 of hydrogen is $\alpha^{(2)} = 3.49 \times 10^{-13}$ cm$^3$ s$^{-1}$ for a typical electron temperature of 7000°, and $4\pi R^2 N_L$ is the rate Lyman continuum photons are emitted by the star. Interpolation between the non–LTE models of Mihalas (1972) with no line blanketing gave $N_L = 3.9 \times 10^{23}$ photons cm$^{-2}$ s$^{-1}$ for $T_{\rm eff} = 34{,}000°$ and $\log g = 4.0$. Comparison of LTE blanketed and unblanketed models showed that multiplication by a factor 1.55 is needed to correct for ultraviolet line blanketing, so that $N_L = 6.0 \times 10^{23}$ photons cm$^{-2}$ s$^{-1}$ and therefore $n_{\rm H} = 5.5$ cm$^{-3}$ in the H II region. The predicted Hα emission measure $EM = \int n_e^2 dl$ is then 910 cm$^{-6}$ pc, which would be reduced to 505 cm$^{-6}$ pc by interstellar absorption of $A_\alpha = 2.0\, E_{B-V}$. However, the observed value of about 190 cm$^{-6}$ pc found by Reynolds *et al.* (1974) indicates that $n_e$ is only 3.4 cm$^{-3}$ and the adopted $R^2 N_L$ is too large by a factor 2.7, probably as a result of absorption of the ionizing photons by dust in the H II region and errors in the calculation of $N_L$. Herbig (1968) obtained EM values of 70 to 350 and $n_e = 3$ from his interpretation of the 400-Hz continuum flux. The column density of ionized hydrogen corresponding to $n_e = 3.4$ is $N(\text{H II}) = 1.6 \times 10^{20}$ cm$^{-2}$ along a radius of the Strömgren sphere. If all the material were in clumps of constant density filling a fraction *f* of the line of sight, $n_e = 3.4 f^{-1/2}$ cm$^{-3}$ and $N(\text{H II}) = 1.6 \times 10^{20} f^{1/2}$ cm$^{-2}$. It was assumed that any H II region outside the Strömgren sphere would have a lower $n_e$ and hence would contribute little to the Hα emission. However, there still could be a significant H II column density in such regions.

In order to estimate the radiation density outside the H II region between 912 and 3000 Å, the LTE blanketed models of Kurucz, Peytremann, and Avrett (1972) are the most appropriate. The emergent flux $\pi F_\nu$ for $T_{\rm eff} = 34{,}000°$ and $\log g = 4.0$ was reduced by one-half the extinction of York *et al.* (1973) and converted to an energy density $u_\nu$ at *r* pc from the star, as listed in column (4) of table 9. Extrapolation of the extinction curve shows that only a small fraction of the total absorption to ζ Oph could provide the attenuation of the Lyman continuum photons within the Strömgren sphere. Black and Dalgarno (1973*a*) assumed that both the H I and $H_2$ toward ζ Oph were located in the same cloud and found that $u_\lambda = 5.6 \times 10^{-16}$ ergs cm$^{-3}$ A$^{-1}$ or $u_\nu = 1.87 \times 10^{-28}$ erg cm$^{-3}$ Hz$^{-1}$ was required at 1000 Å near the center of the cloud to reproduce the populations of the $H_2$ rotational levels observed with *Copernicus*. In this case the cloud would be only 23 pc from the star.

TABLE 9

STELLAR FLUX AND RADIATION FIELD

| $\lambda$ (Å) | $\pi F_\nu$* ($10^{-3}$ ergs cm$^{-2}$ s$^{-1}$ Hz$^{-1}$) | $\frac{E(\lambda - V)}{E(B - V)}$† | $r^2 u_\nu(\zeta$ Oph) ($10^{-25}$ pc$^2$ erg cm$^{-3}$ Hz$^{-1}$) | $u_\nu$(WJ1)‡ ($10^{-29}$ ergs cm$^{-3}$ Hz$^{-1}$) |
|---|---|---|---|---|
| 930..... | 6.74 | 17.7 | 0.40 | 0.25 |
| 975..... | 9.98 | 15.5 | 0.81 | 0.75 |
| 1025..... | 10.58 | 13.4 | 1.17 | 1.25 |
| 1075..... | 10.65 | 11.5 | 1.57 | 1.75 |
| 1125..... | 10.73 | 9.8 | 2.02 | 2.15 |
| 1175..... | 10.50 | 8.9 | 1.98 | 2.55 |
| 1220..... | 9.90 | 8.0 | 2.44 | 3.10 |
| 1270..... | 10.18 | 7.1 | 2.85 | 4.20 |
| 1325..... | 9.94 | 6.5 | 3.05 | 5.20 |
| 1375..... | 9.45 | 6.1 | 3.07 | 6.10 |
| 1422..... | 9.25 | 5.8 | 3.14 | 6.85 |
| 1482..... | 9.16 | 5.5 | 3.26 | 7.75 |
| 1547..... | 8.05 | 5.3 | 2.94 | 8.70 |
| 1598..... | 8.59 | 5.1 | 3.24 | 8.35 |
| 1649..... | 8.35 | 5.0 | 3.19 | 7.50 |
| 1730..... | 7.98 | 4.9 | 3.10 | 6.35 |
| 1830..... | 7.54 | 4.9 | 2.93 | 5.00 |
| 1930..... | 7.13 | 5.0 | 2.73 | 4.50 |
| 2015..... | 6.80 | 5.5 | 2.42 | 4.50 |
| 2100..... | 6.65 | 5.8 | 2.26 | 4.50 |
| 2150..... | 6.48 | 5.95 | 2.15 | 4.50 |
| 2200..... | 6.29 | 5.8 | 2.14 | 4.50 |
| 2300..... | 5.96 | 5.3 | 2.18 | 4.70 |
| 2400..... | 5.64 | 4.9 | 2.19 | 5.45 |
| 2482..... | 5.37 | 4.1 | 2.35 | 6.05 |
| 2557..... | 5.20 | 3.8 | 2.37 | 6.60 |
| 2660..... | 4.93 | 3.2 | 2.46 | 7.25 |
| 2770..... | 4.67 | 2.9 | 2.43 | 7.90 |
| 2870..... | 4.44 | 2.7 | 2.38 | 8.50 |
| 2970..... | 4.23 | 2.4 | 2.37 | 9.00 |

* Kurucz, Peytremann, and Avrett (1972); $T_{\rm eff} = 34{,}000°$, $\log g = 4.0$.

† York *et al.* (1973).

‡ de Boer, Koppenaal, and Pottasch (1973).

For comparison, the final column of table 9 lists the average interstellar radiation field derived by Witt and Johnson (1973) with the WJ1 extrapolation shortward of 1200 Å used by de Boer, Koppenaal, and Pottasch (1973) for their calculations of ionization cross sections. At $r = 70$ pc from $\zeta$ Oph, the model gives the same radiation density as WJ1 within a factor of 1.5 between 930 and 2500 Å. Consequently, for ionization calculations in the clouds, two extremes were adopted: (*a*) clouds at $r \geq 100$ pc from $\zeta$ Oph, where the WJ1 interstellar radiation field is appropriate, and (*b*) clouds at $r = 15$ pc, where the radiation averages about 20 times the standard WJ1 distribution and is adequate to populate the excited rotational levels of $H_2$. In this way it was possible to use either (*a*) the photoionization rates $\Gamma$ for WJ1 tabulated by de Boer *et al.* (1973) or (*b*) 20 times these values. In (*b*) the rates used for Mg I, Si I, and Fe I may be a little high, and those for Al I, S I, and C I slightly low. An additional case might have been considered in which the ionization is due to the WJ1 field attenuated by the ultraviolet absorption corresponding to $E_{B-V} = 0.10$, which is half the excess extinction in the $\zeta$ Oph cloud over the average $E_{B-V}$ of 0.61 kpc$^{-1}$ (Spitzer 1968). However, since there is still radiation from the star, WJ1 remains a reasonable lower limit for the ionizing flux because the contribution from $\zeta$ Oph compensates for the reduction in WJ1 out to 100 pc from the star at 2028 Å where Ca I is ionized and out to 90 pc at 1101 Å where C I is ionized. Even at 200 pc, the flux at the Ca I limit would be reduced by a factor of only 0.7 and at the C I limit by a factor 0.5.

## VI. IONIZATION IN THE H I CLOUDS

In the interstellar gas, the volume densities $n_r$ and $n_{r+1}$ of successive ion stages of an element are related by

$$\frac{n_{r+1} n_e}{n_r} = \frac{\Gamma}{\alpha_t}, \tag{2}$$

where $\Gamma$ is the photoionization cross section and $\alpha_t$ is the total radiative recombination coefficient to all levels. This equation assumes that there are no molecular reactions which affect the ion populations significantly. In tables 10 and 11, which are appropriate for the H I clouds, $\Gamma$ is quoted for the WJ1 interstellar radiation field following the calculations of de Boer *et al.* (1973), with Li I added by a private communication from de Boer. In the case of Cl I, the $\Gamma$ is a rough estimate by Jura (1974*a*). The recombination coefficients for $T = 56°$ K were obtained from Aldrovandi and Pequignot (1973) when available, or from Seaton

TABLE 10

CALCULATION OF THE ELECTRON DENSITY

| Element | I.P. (eV) | Γ(WJ1)* ($s^{-1}$) | $\alpha_t(56°)$ ($cm^3\ s^{-1}$) | log $N_r$ ($cm^{-2}$) | log $N_{r+1}$ ($cm^{-2}$) | $n_{r+1}/n_r$ | $\langle n_e \rangle$ ($cm^{-3}$) |
|---|---|---|---|---|---|---|---|
| C I | 11.260 | $1.4 \times 10^{-10}$ | $1.2 \times 10^{-11}$ | 15.56 | 16.80–17.15 | 17.4–39 | 0.67–0.30 |
| Mg I | 7.646 | $7.8 \times 10^{-11}$ | $1.2 \times 10^{-11}$ | 14.15 | 14.91–15.27 | 5.8–13.2 | 1.13–0.49 |
| Al I | 5.986 | $2.1 \times 10^{-9}$ | $1.2 \times 10^{-11}$ | < 10.21 | 12.09–12.41 | > 76 | < 2.3 |
| Si I | 8.151 | $3.6 \times 10^{-9}$ | $1.3 \times 10^{-11}$ | < 12.58 | 14.80–15.30 | > 166 | < 1.7 |
| S I | 10.360 | $1.3 \times 10^{-9}$ | $1.1 \times 10^{-11}$ | 13.93 | 15.86–16.24 | 85–204 | 1.39–0.58 |
| Cl I | 12.967 | $1.2 \times 10^{-10}$ | $1.2 \times 10^{-11}$ | 14.03 | 13.08–13.63 | 0.11–0.40 | 90–25 |
| Ca I(−14) | 6.113 | $3.7 \times 10^{-10}$ | $8.6 \times 10^{-12}$ | 9.72 | 11.64–11.73 | 83–102 | 0.52–0.42 |
| Ca I(−28) | 6.113 | $3.7 \times 10^{-10}$ | $8.6 \times 10^{-12}$ | < 9.11 | 11.05–11.14 | > 87 | < 0.49 |
| Ca I total | 6.113 | $3.7 \times 10^{-10}$ | $8.6 \times 10^{-12}$ | 9.72–9.82 | 11.74–11.83 | 83–129 | 0.52–0.33 |
| Ti I(−28) | 6.82 | $4.5 \times 10^{-10}$ | $1.2 \times 10^{-11}$ | < 11.25 | 11.42–11.54 | > 1.48 | < 25. |
| Mn I | 7.435 | $1.1 \times 10^{-10}$ | $1.2 \times 10^{-11}$ | < 11.58 | 13.26–13.33 | > 48 | < 0.19 |
| Fe I | 7.870 | $3.0 \times 10^{-10}$ | $1.2 \times 10^{-11}$ | 11.52 | 14.48–14.64 | 910–1320 | 0.027–0.019 |

* For the WJ1 interstellar radiation field of de Boer *et al.* (1973). At 22 pc from ζ Oph each Γ and the corresponding $\langle n_e \rangle$ would be about 10 times larger.

(1951) or Herbig (1968) scaled for temperature according to equation 36 of Seaton (1959). The kinetic temperature of 56° K was derived by Spitzer, Cochran, and Hirshfeld from the ratio of ortho to parahydrogen in the rotational levels $J'' = 1$ and 0 toward ζ Oph. If the best fit for all levels up to $J'' = 3$ is more appropriate, $T = 94°$ K, which is near the likely upper limit for a typical H I cloud. Since $\alpha_t$ varies at $T^{-0.7}$, the recombination coefficient should be decreased by a factor of about 1.4 and the derived electron density increased by the same factor. Alternatively, if $T = 19°$ K, as found from one interpretation of the fine-structure populations of C I, $\alpha_t$ would be reduced by a factor 2.1. If the cloud is close to the star, each Γ and $n_e$ could be up to 20 times larger.

Since there is evidence that the neutrals and first ions of many elements may be distributed differently along the line of sight, the values of $n_e$ in table 10 derived from the column densities cannot be interpreted directly as electron densities. However, Jenkins (1974) has shown that if the abundance ratio of two elements is independent of position, and the density of the first ion $n_{+1}$ is greater than the neutral $n_0$ in each case, the mean $n_e$ obtained from equating $n_{+1}/n_0$ to $N_{+1}/N_0$ should be the same for the two elements. Such appears to be the case for C, Mg, S, and Ca, with $n_e \sim 0.7\ cm^{-3}$ within a factor 2, while Fe and possibly Mn give a value 30 times smaller. The results for Cl will be discussed at the end of this section.

For the general interstellar field, the $n_e$ derived from Ca II/Ca I agrees with the value found by de Boer and Pottasch (1974) and by Shulman *et al.* (1974), but it is larger by a factor of 5 or 10 than the calculations of White (1973), or Field (1974*a*) who adopted lower values for Γ than now seem reasonable. Jura (1974*b*) has called attention to the possibility that dielectronic recombination of Ca II could make Ca I the dominant ion stage in an H II region. However, a similar effect should occur for Mg I unless the temperature happens to lie in a narrow range around 8000° K, but not for C I and S I. Furthermore, the Ca I line has a radial velocity of $-7.8\ km\ s^{-1}$ relative to the Strömgren sphere around ζ Oph. Any comparison of C, Mg, or S with Ca should use the total Ca II in all clouds since figure 3 suggests that the other ions are present in more than one cloud. Nevertheless, the agreement of Ca with C, Mg, and S may be accidental, since the severe depletion of calcium could result in a special distribution over the clouds, as happens for titanium. It was noted in the previous section that Ca II did not agree with the other curves of growth, even if total equivalent widths were used.

It was assumed that $n_e = 0.7$ was appropriate for calculating the column densities of the unobservable Li II, Na II, and K II, as shown in table 11. The ratio Ca III/Ca II also was included to demonstrate that this fraction must be less than unity unless $n_e < 0.03\ cm^{-3}$. The last column of table 11 gives total column densities in the H I regions. If the radiation field were stronger than WJ1, $n_e$ would be proportionately larger, but the number ratios in table 11 would be unaffected unless the stellar energy distribution deviated markedly from that predicted in table 9.

TABLE 11

ABUNDANCES OF UNOBSERVED IONS IF $\langle n_e \rangle = 0.7\ cm^{-3}$

| Element | I.P. (eV) | Γ(WJ1) ($s^{-1}$) | $\alpha_t(56°)$ ($cm^3\ s^{-1}$) | log $N_r$ ($cm^{-2}$) | $n_{r+1}/n_r$ | log $N_{r+1}$ | log($N_r + N_{r+1}$) |
|---|---|---|---|---|---|---|---|
| Li I | 5.392 | $1.8 \times 10^{-10}$ | $8.7 \times 10^{-12}$ | 9.36 | 30. | 10.83 | 10.85 |
| Na I | 5.139 | $1.8 \times 10^{-11}$ | $8.4 \times 10^{-12}$ | 13.86 ± 0.1 | 3.1 | 14.35 ± 0.1 | 14.47 ± 0.1 |
| K I | 4.341 | $5.4 \times 10^{-11}$ | $8.0 \times 10^{-12}$ | 11.90–12.39 | 9.6 | 12.88–13.37 | 12.91–13.40 |
| Ca II | 11.871 | $1.5 \times 10^{-12}$ | $5.0 \times 10^{-11}$ | 11.74–11.83 | 0.043 | 10.37–10.46 | 11.76–11.85 |

Previous investigators (White 1973; Traub and Carleton 1973; Field 1974*a*, *b*; de Boer and Pottasch 1974; Shulman *et al.* 1974) found similar Na II densities and showed that Ca III added little to the total Ca abundance. However, the present determinations of Li II and K II are considerably smaller, mainly as a result of better estimates for the ionization cross sections. If the ionization of Fe I were more appropriate for the calculations of table 11, the values of $n_{r+1}/n_r$ would be a factor 30 larger.

The $\langle n_e \rangle$ derived in table 10 is an average value which may not be relevant for other calculations such as the population of excited fine-structure levels. However, there must be a cloud with $n_e$ at least this large to produce the observed amounts of neutrals. If a majority of the C II, Mg II, etc., is not in the cloud with the C I and Mg I, the true $n_e$ for this cloud would be proportionately higher. Jura (1974*b*) has concluded that the hydrogen ionization rate $\zeta_H$ due to cosmic rays or X-rays at the center of a dense cloud must be less than $5 \times 10^{-17}$ s$^{-1}$ per H nucleus to provide the proper amount of $H^+$ needed for the production of the observed HD. Similar limits on $\zeta_H$ have been obtained by Black and Dalgarno (1973*a*) and by O'Donnell and Watson (1974). Furthermore, Glassgold and Langer (1973) have noted that $\zeta_H \sim 10^{-16}$ s$^{-1}$ would destroy the $H_2$. With such limits on $\zeta_H$, and temperatures $\leq 56°$, carbon is a more important source of electrons than hydrogen. If the ratio C II/H $= 7 \times 10^{-5}$ in table 7 is typical, $n_e \geq 0.7$ corresponds to $n_H \geq 10^4$ cm$^{-3}$; or if there is no carbon depletion, $n_H \geq 2 \times 10^3$. Since the underabundance appears to be real, the higher $n_H$ is adopted here. Then the fractional ionization $n_e/n_H = 7 \times 10^{-5}$. The total column density of singly ionized carbon $N(\text{C II}) = 10^{17}$ cm$^{-2}$ places an upper limit of about 0.05 pc on the thickness of the cloud. Shulman *et al.* (1974) also concluded from Ca I/Ca II that the hydrogen density in one cloud must be within a factor 2 of $10^4$ cm$^{-3}$. Herbig (1968) had discovered the need for a thin dense cloud in the direction of $\zeta$ Oph, but his value of $500 \leq n_H \leq 900$ cm$^{-3}$ was lower due to his assumption that Na and C were present with solar abundances.

The large population of Cl I relative to Cl II was predicted by Jura (1974*a*), who considered the reactions of both Cl and $Cl^+$ in the presence of $H_2$ as well as photons and electrons. Two of the products, HCl and $HCl^+$, react with photons and electrons, respectively, to produce neutral chlorine at a faster rate than the photons between 911.8 and 956.1 Å can ionize it. Therefore, the high $n_e$ derived for this element in table 9 is not meaningful. The upper limit on HCl in table 8 is a factor $\sim 30$ below Jura's estimate for a cloud with $n_H = 20$ cm$^{-3}$, but it is consistent with the model having $n_H = 2500$ cm$^{-3}$ proposed by Dalgarno *et al.* (1974), provided the observed Cl II lies in a different region.

## VII. EXCITED LEVELS, PHYSICAL CONDITIONS, AND THE RATE OF COOLING

The observed populations of the excited fine-structure levels of C I, C II, N II, and Si II, along with the limits for O I and Fe II, must place certain constraints on the physical conditions in the gas toward $\zeta$ Oph. Also, since the principal cooling mechanism in the gas is the infrared emission from these levels and the lower excited rotational levels of $H_2$, the cooling rate can be deduced directly.

### *a) Excited Atomic Levels*

As described by Bahcall and Wolf (1968), the relative populations of the fine-structure levels in the ground term are governed by the equations of statistical equilibrium which take account of the transitions induced by both photons and particle collisions as well as the spontaneous radiation from the upper levels. Decays from the high levels populated by the absorption of ultraviolet photons were included for C I by de Boer and Morton (1975), but the effect was ignored for the other species except N II and Si II in the Strömgren sphere. In the H II regions it was assumed that $n_e = n_p$ and $n_{H\,I} = n_{H_2} = 0$, while in H I regions $n_e = 7 \times 10^{-5} n_H$ from the observed abundance of C II, and $n_p = 1.4 \times 10^{-6} n_H$ from the upper limit $\zeta_H \leq 5 \times 10^{-17}$ for the hydrogen ionization rate from cosmic rays and hard X-rays (Jura 1974*b*). In the latter regions proton collisions were included for the neutrals and electron collisions for the ions, but in both cases the H atoms and molecules were more important. Dalgarno and McCray (1972, p. 390) estimated that the collision cross section for an $H_2$ molecule is about one-fourth that of an H atom so that the calculations

TABLE 12

EXCITED FINE-STRUCTURE LEVELS

| Ion | $g_1$ | $g_2$ | $g_3$ | $T_{12}$ (° K) | $T_{13}$ (° K) | $A_{21}$ (s$^{-1}$) | $A_{31}$ (s$^{-1}$) | $A_{32}$ (s$^{-1}$) | log $(N_2/N_1)$ | log $(N_3/N_1)$* |
|---|---|---|---|---|---|---|---|---|---|---|
| C I..... | 1 | 3 | 5 | 23.60 | 62.44 | $7.93 \times 10^{-8}$ | $2.00 \times 10^{-14}$ | $2.68 \times 10^{-7}$ | $-0.30 \pm 0.20$ | $-0.95 \pm 0.20$ |
| C II..... | 2 | 4 | | 91.25 | ... | $2.36 \times 10^{-6}$ | ... | ... | $-2.0 \pm 0.1$ | ... |
| N II..... | 1 | 3 | 5 | 70.6 | 188.9 | $2.13 \times 10^{-6}$ | $1.30 \times 10^{-12}$ | $7.48 \times 10^{-6}$ | ... | $-1.7 \pm 1.0$ |
| O I..... | 5 | 3 | 1 | 228.0 | 325.9 | $8.95 \times 10^{-5}$ | $1.00 \times 10^{-10}$ | $1.70 \times 10^{-5}$ | $< -44$ | $< -4.9$ |
| Si II..... | 2 | 4 | | 413.4 | ... | $2.13 \times 10^{-4}$ | ... | ... | $-2.9 \pm 0.6$ | ... |
| Fe II..... | 10 | 8 | 6 | 553.6 | 960.6 | $2.1 \times 10^{-3}$ | $1.5 \times 10^{-9}$ | $1.6 \times 10^{-3}$ | $< -2.3$ | ... |

* In the case of C I, the ratio $N_3/N_2$ is better determined with log $(N_3/N_2) = -0.65 \pm 0.15$.

were carried out with an effective hydrogen density

$$n'_{\rm H} = n_{\rm H\,I} + 0.25 n_{\rm H_2} = n_{\rm H}(1 - 7F/8)\,, \qquad (3)$$

where $n_{\rm H} = n_{\rm H\,I} + 2n_{\rm H_2}$, $F = 2n_{\rm H_2}/n_{\rm H}$, and $0 \leq F \leq 1$. In the calculations for ζ Oph, $F = 0.6$. Table 12 lists the statistical weights $g_1$, $g_2$, $g_3$, the excitation temperatures $T_{12}$, $T_{13}$, and the spontaneous transition probabilities $A_{21}$, $A_{31}$, $A_{32}$ for the fine-structure levels, along with the ranges of population ratios $N_2/N_1$ and $N_3/N_1$ from table 7. The atomic parameters, including collision rates, were obtained from Wiese, Smith, and Glennon (1966), Bahcall and Wolf (1968), Dalgarno and McCray (1972), and Smith and Weise (1973).

As discussed by de Boer and Morton (1975), if $n_{\rm H} \sim 10^4$ cm$^{-3}$ derived from the ionization calculations of § VI is the correct density in the region containing the majority of the C I, the ratios C I**/C I* and C I*/C I constrain the kinetic temperature to $T = 19°$ K, provided $n_{\rm H_2} \sim n_{\rm H\,I}$ and the cloud is at least 100 pc from ζ Oph. At 15 pc from the star, at the edge of the Strömgren sphere, the density would be 20 times higher but the temperature would be only a degree lower since the C I population ratios depend mainly on the temperature for $n_{\rm H} \geq 10^4$ cm$^{-3}$. The range in pressure $nT$ is $1.2 \times 10^5$ to $2.4 \times 10^6$ cm$^{-3}$ deg. In either case, the temperature derived from the C I would make C II*/C II $= 10^{-2}$, consistent with the observed ratio.

However, most of the rotationally excited $H_2$ must be in another cloud since Dalgarno, Black, and Weisheit (1973) have shown that charge-exchange collisions with protons cause the population ratio between $J'' = 0$ and 1 to be determined by the kinetic temperature. There must be a second cloud of $H_2$ with $T$ between the 56° obtained from the observed populations of $J'' = 0$ and 1 and the 115° found from $J'' = 1$ and 2. Extrapolation of the latter two points on the graph of Spitzer and Cochran (1973) gave $N_{\rm H_2} = 6.2 \times 10^{19}$ cm$^{-2}$ in $J'' = 0$ in a cloud at 115°, leaving at most $2.3 \times 10^{20}$ cm$^{-2}$ in this state in the 19° cloud and negligible amounts in $J'' = 1$, 2, and 3. Up to 55 percent of the total $H_2$ toward ζ Oph could be in the cold cloud. The temperature of 327° found from $J'' = 3$ to 6 probably results from the mechanisms discussed by Spitzer and Zweibel (1974), which populate these levels rather than any physical value of particle velocities. Relatively little HD is likely to be present in the cold cloud since the reaction $H^+ + D \rightarrow H + D^+$ required to form this molecule has a potential barrier of 0.0036 eV or 42°. According to figure 3, the cold, dense cloud containing the C I and as much as 80 percent of the $H_2$ in $J'' = 0$ has a radial velocity similar to the hotter cloud with the HD and the excited levels of $H_2$. It is possible that these parameters represent inner and outer parts of the same cloud. For pressure equilibrium with $T \sim 115°$ and $F = 0.6$ in the second cloud, $n_{\rm H} \sim 2 \times 10^3$, or $4 \times 10^4$ cm$^{-3}$ if the cloud is only 15 pc from the star. The lower density is consistent with the model of the ζ Oph cloud proposed by Black and Dalgarno (1973*a*) requiring $n_{\rm H_2} = 1560$ cm$^{-3}$ and $n_{\rm H\,I} = 880$ cm$^{-3}$ to explain the HD density and the population of $H_2$ in $J'' = 6$.

If carbon is distributed like the $H_2$, at least 45 percent should be in the warmer region, where $T \geq 56°$ and $n_{\rm H}T \sim 2 \times 10^5$ cm$^{-3}$ deg, with the result that C II*/C II $\geq 0.1$ compared with the observed ratio of 0.008 to 0.0125. Therefore, the C II must be less concentrated in the region of the excited $H_2$ or the density there cannot be much more than $2 \times 10^2$ cm$^{-3}$. Jura (1974*c*) has concluded that this density would be too low to produce the required populations of excited $H_2$. Alternatively, it is possible that the use of the same curve of growth for both C II* and C II in table 7 has given an incorrect ratio. Smith (1972) found C II*/C II ~ 1.0 from a rocket spectrum, and consequently he had to assume that all the C II* and much of the C II was in the Strömgren sphere with a density of 220 cm$^{-3}$, implying rather extreme clumpiness to produce the observed emission measure discussed in § V. The points in figure 3 indicate that some of both C II and C II* must be in a cloud at −25.5 or −27.6 km s$^{-1}$; but since the lines are on the saturated Doppler part of the curve of growth, a small fraction in this cloud could easily cause a large shift in the center of a profile.

The absence of O I* implies $n_{\rm H} \leq 3 \times 10^2$ cm$^{-3}$ at $T = 115°$ and $n_{\rm H} \leq 7 \times 10^3$ at $T = 56°$. Thus it seems more likely that the O I, like the C II, may be concentrated in the cold cloud where O I*/O I would be only $1.5 \times 10^{-9}$. Repeated scans searching for the O I* line would be useful to see if the ratio really is much below the present limit of $4 \times 10^{-5}$. Although O I* was not found, Si II* was easily detected in spite of its much higher excitation temperature. The Si II* cannot be formed in the 19° cloud. The lower limit on Si II*/Si II requires $n_{\rm H} \geq 3 \times 10^3$ cm$^{-3}$ if $T = 115°$ and $n_{\rm H} \geq 1.5 \times 10^4$ cm$^{-3}$ if $T = 56°$. It is clear that the Si II* cannot be present with the O I; but if most of the Si II were with the excited $H_2$ while the O I were mostly in the cold cloud, the Si II* abundance could be consistent with the densities derived from the assumption of pressure equilibrium.

The H II regions, where the O I should be fully ionized, is a more likely source of the Si II*, as pointed out by Jenkins (1974). Both N II** and N II also must lie where photons can ionize hydrogen, while Si II can occur in both H I and H II regions. Since electron collisions must be the primary cause of these excitations, the observed column densities ought to provide some information about the mean $n_e$ and hence the fraction of Si II in H II regions. Unfortunately the large uncertainty in $N$(N II) leaves $n_e$ poorly determined and consequently Si II*/Si II. The unknown filling factor in the Strömgren sphere prevents a direct calculation from the $n_e$ obtained from the emission measure. Nonetheless, the similarity in velocities in figure 3 between Si II and both O I and N I suggest that the Si II comes mainly from the H I clouds.

The observed column density of N II** does provide a direct measurement of the average abundance $X = N$(N II)/$N$(H) in the H II regions, provided $X$ does not vary greatly along the path. In the H II regions it is

reasonable to assume that H II and N II are the dominant ions states, and that the small population in N II** is governed mainly by collisional excitation with electrons and spontaneous radiative decays. Therefore,

$$n(\text{N II}^{**})(A_{32} + A_{31}) = n(\text{N II})n_e\langle\sigma v\rangle_{13} \quad (4)$$

and

$$N(\text{N II}^{**}) = \frac{\langle\sigma v\rangle_{13}}{A_{32} + A_{31}} X \int_{\text{center}}^{\text{edge}} n(\text{H II})n_e dl$$

$$= \frac{\langle\sigma v\rangle_{13}}{A_{32} + A_{31}} X \frac{\text{EM}}{2} \text{dex}\,(0.4A_\alpha)\,, \quad (5)$$

where $\langle\sigma v\rangle_{13} = 2.0 \times 10^{-8}\,\text{cm}^3\,\text{s}^{-1}$ for $T = 7000°$, and changes little for other temperatures likely to occur within an H II region. Consequently, for an emission measure $\text{EM} = 190\,\text{cm}^{-6}\,\text{pc}$ and $\log N(\text{N II}^{**}) = 14.03 \pm 0.20$, $\log(\text{N II/H}) = -4.12 \pm 0.20$. A similar calculation with $\log N(\text{Si II}^{**}) = 12.18 \pm 0.32$ gave $\log(\text{Si II/H}) = -5.81 \pm 0.32$. According to the discussion by Spitzer and Jenkins (1975), correction for the effects of cascading from higher levels excited by ultraviolet photons decreases the abundances to $-4.21 \pm 0.20$ for N II and $-6.13 \pm 0.32$ for Si II.

### b) *Cooling Rate in* H I *Clouds*

In a steady state, the column density $N$ of an excited fine-structure level is related directly to the rate $dE/dt$ at which energy is radiated from the interstellar gas. If $A$ is the Einstein coefficient for spontaneous emission, and $1/\lambda$ is the wavenumber for the transition, then

$$dE/dt = ANhc/\lambda\,. \quad (6)$$

The relevant quantities have been listed in table 13 with $dE/dt$ normalized to the total number of hydrogen nuclei $N_{\text{H}} = 1.36 \times 10^{21}\,\text{cm}^{-2}$. The values of $A$ were obtained from Field, Somerville, and Dressler (1966), Wiese *et al.* (1966), or Dalgarno and Wright (1972). The ortho-para transitions in $H_2$ and the electric-quadrupole rates from the highest to the lowest levels in O I and C I (see table 12) can be ignored. The ratio of statistical weights requires that $N(\text{O I}^{**})$ be less than $N(\text{O I}^{*})/3$. The cooling due to Si II* is negligible even if it is all in the H I regions. The excited levels of N II have been omitted because they originate in the H II regions, where the cooling is dominated by the recombination lines of hydrogen. Radiation from the $H_2$ levels with $J'' \geq 4$ does not cool the gas because those levels probably have been populated in the formation process or by transitions from higher vibrational levels which have been excited by photons (Spitzer and Zweibel 1974). Clearly the dominant cooling agent is the C II*, with smaller contributions from $H_2$ and possibly O I* depending on how far it lies below the upper limit. Penston (1974) already has noted the importance of C II* in a similar calculation based on the earlier *Copernicus* data. Presumably this energy loss of about $3 \times 10^{-26}\,\text{erg}^{-1}$ per H nucleus (or up to $5 \times 10^{-26}$ if O I* is important) is balanced by inputs to the kinetic energy of the gas from photoemission from the grains as well and the formation of $H_2$.

## VIII. ELEMENT ABUNDANCES

### a) H I *Regions*

The abundances of the neutrals and first ions which are likely to originate mainly in H I clouds have been discussed in a separate paper by Morton (1974). Since the radial velocities in figures 3 and 4 imply that most of the Mg II, Si II, Fe II, etc., probably lie in the H I regions, the contributions of the H II regions to the first ions have been ignored, except for N II which cannot be coincident with the H I. The results relative to $N_{\text{H I}} + 2N_{\text{H}_2}$ have been plotted in figure 7 where a point below the zero line indicates an element is depleted with respect to the Sun. In most cases the length of a bar accounts for $6 \leq b \leq 7\,\text{km s}^{-1}$ in the curve of growth and possible errors in $W_\lambda$ and $f$. All the elements analyzed showed significant depletions except S and Zn, which could be normal within the plausible uncertainties, and Be and Co, which did not have tight enough upper limits. The underabundances of Cl and Ar were somewhat uncertain due to possible

TABLE 13

COOLING RATE IN H I REGIONS

| Particle | $J_u$ | $J_l$ | $1/\lambda$ (cm$^{-1}$) | $A_{ul}$ (s$^{-1}$) | $N$ (cm$^{-2}$) | $N_{\text{H}}^{-1}dE/dt$ (ergs s$^{-1}$ H atom$^{-1}$) |
|---|---|---|---|---|---|---|
| $H_2(v'' = 0)$ ..... | 1 | 0 | 118.49 | $7 \times 10^{-21}$ | $1.3 \times 10^{20}$ | $1.6 \times 10^{-35}$ |
| | 2 | 0 | 354.39 | $2.95 \times 10^{-11}$ | $3.6 \times 10^{18}$ | $5.5 \times 10^{-27}$ |
| | 2 | 1 | 235.90 | $8 \times 10^{-19}$ | $3.6 \times 10^{18}$ | $1.0 \times 10^{-35}$ |
| | 3 | 1 | 587.05 | $4.77 \times 10^{-10}$ | $1.2 \times 10^{17}$ | $4.9 \times 10^{-27}$ |
| HD($v'' = 0$) ..... | 1 | 0 | 89.23 | $2.54 \times 10^{-8}$ | $< 3.2 \times 10^{13}$ | $< 1.1 \times 10^{-29}$ |
| C I* ..... | 1 | 0 | 16.40 | $7.93 \times 10^{-8}$ | $1.1 \times 10^{15}$ | $2.1 \times 10^{-28}$ |
| C I** ..... | 2 | 1 | 27.00 | $2.68 \times 10^{-7}$ | $2.5 \times 10^{14}$ | $2.6 \times 10^{-28}$ |
| C II* ..... | 3/2 | 1/2 | 63.42 | $2.36 \times 10^{-6}$ | $1.0 \times 10^{15}$ | $2.2 \times 10^{-26}$ |
| O I* ..... | 1 | 2 | 158.5 | $8.95 \times 10^{-5}$ | $< 7.6 \times 10^{12}$ | $< 1.6 \times 10^{-26}$ |
| O I** ..... | 0 | 1 | 68.0 | $1.70 \times 10^{-5}$ | $< 2.5 \times 10^{12}$ | $< 4.2 \times 10^{-28}$ |
| Si II* ..... | 3/2 | 1/2 | 287.32 | $2.13 \times 10^{-4}$ | $\sim 1.5 \times 10^{12}$ | $1.3 \times 10^{-28}$ |
| Total ..... | | | | | | $3.3 \times 10^{-26}$ |

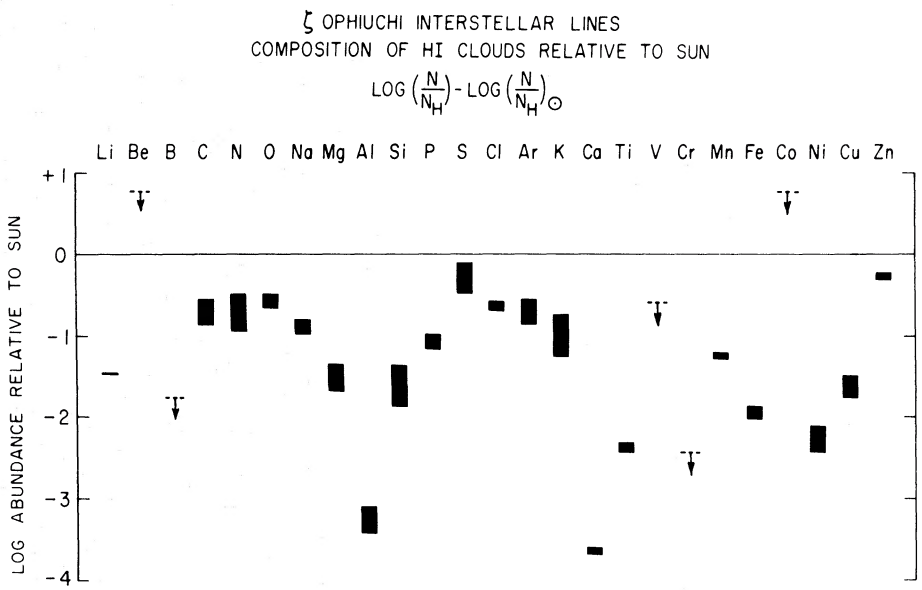


FIG. 7.—Composition of H I clouds in the direction of ζ Oph, relative to the Sun. An element lying below the horizontal line is depleted compared with its solar system abundance. Ions such as N II and Si III, which are expected to be entirely in H II regions, were not included. The lengths of the vertical bars mainly indicate the uncertainties in the curve of growth, though in some cases the bars were lengthened when errors in equivalent widths or *f*-values were important.

errors in the adopted solar values. Also, it should be remembered that any errors in the calculated *f*-values of Cr II, Co II, Ni II, and Cu II would change the plotted positions for these elements. The correlation of depletion with increasing condensation temperature has been discussed by Field (1974*a*, *b*) and by Morton (1974). The difficulty caused by the absence of the B II line has been noted by Morton *et al.* (1974).

### *b*) H II *Regions*

Presumably the H II regions are the source of all ions like N II, Al III, Si III, etc., which require photon energies above 13.5 eV. Substantial quantities of lower ion stages such as C II, Al II, Si II, etc., also could be present without increasing the depletions in figure 7 for the H I regions, which have 10 times the number of H nuclei. Calculations of the ionization equilibrium in Strömgren spheres of uniform density by Thuan (1975) do show that the contributions of C I, Si I, and S I are negligible while N I/N II could be ~0.1. Table 14 summarizes the available information on the abundances in the ζ Oph Strömgren sphere, for which $N$(H II) was derived in § V from the emission measure and the assumption of no extreme clumping. The column densities of N II and Si II were obtained directly from the populations of the excited fine-structure levels discussed in § VII. For the other first ions only upper limits were available for the observed densities in table 14. The velocity of −28 km s$^{-1}$ found for Ti II eliminates that component from consideration. The low populations of N III and Si IV show that the unobservable N IV, Al IV, etc. probably do not contribute much. Any Al III, Si III, etc., located in H II regions outside the Strömgren sphere would only reduce the totals in table 14. Errors also are possible in V III, Cr III, and Fe III because of the *f*-values adopted from Kurucz (1974). Calculations of the actual contributions of P II, S II, and Fe II could

TABLE 14

ELEMENT ABUNDANCES IN THE STRÖMGREN SPHERE

| Ion | Column Density (cm$^{-2}$) log $N$(II) | log $N$(III) | log $N$(IV) | log $N$(total) | log $(N/N_H)_\odot$ + 12.0 | log $(N/N_H)$ − log $(N/N_H)_\odot$ |
|---|---|---|---|---|---|---|
| H..... | 20.20 | ... | ... | 20.20 | 12.00 | 0 |
| N..... | 15.99 ± 0.20 | < 13.94 | ... | 15.83 to 16.23 | 8.06 | −0.43 to −0.03 |
| Al..... | < 12.41 | 12.63 to 12.72 | ... | 12.63 to 12.89 | 6.40 | −1 97 to −1.71 |
| Si..... | 14.07 ± 0.32 | 13.13 to 14.72 | 12.57 to 12.84 | 13.87 to 14.89 | 7.64 | −1.88 to −0.86 |
| P..... | < 13.56 | < 13.06 | ... | < 13.67 | 5.43 | < +0.04 |
| S..... | < 16.24 | 14.70 to 15.00 | ... | 14.70 to 16.26 | 7.21 | −0.71 to +0.85 |
| Ti..... | < 11.00 | < 12.39 | ... | < 12.41 | 4.74 | < −0.53 |
| V..... | < 12.61 | < 12.44 | ... | < 12.83 | 4.10 | < +0.53 |
| Cr..... | < 12.35 | < 13.28 | ... | < 13.33 | 5.70 | < −0.57 |
| Fe..... | < 14.64 | 13.57 to 13.62 | ... | 13.57 to 14.68 | 7.40 | −2.03 to −0.92 |

lower the upper limits significantly for these elements.

The final column of table 14 shows the comparison with the solar abundances of Withbroe (1971). Nitrogen is normal within a factor 2, while Al, Si, Ti, Cr, and Fe show definite evidence of underabundance. Since grains often occur in H II regions, the depletions are not surprising, though the difference in Al between the H I clouds and the Strömgren sphere was not expected.

## IX. SUMMARY OF RESULTS

This paper has combined published ground-based observations of interstellar absorption lines in $\zeta$ Oph with recent far-ultraviolet spectral scans by the *Copernicus* satellite telescope. The tables contain the equivalent widths of 295 lines and upper limits for 33 more in the two regions. There are 45 unidentified lines in the ultraviolet in addition to the numerous diffuse bands known in the visible. Lines due to interstellar Ni, Cu, and Zn were detected for the first time.

Hobbs's (1973*a*) interferometer scans of the visible Na I and Ca II lines have revealed at least six separate clouds. The available velocity information on the ultraviolet lines indicated that the majority of the $H_2$, the HD, and the neutral atoms such as C I, Mg I, S I, and Cl I must be located in the cloud at $V_\odot = -14.4$ km s$^{-1}$ that also has all the detectable K I, Li I, and Fe I and most of the Na I. Other neutrals such as N I, O I, and Ar I, and all first ions except N II, Ca II, and Ti II seem to be present in at least two clouds, one at $-14.4$ or $-12.6$ km s$^{-1}$ with most of the material and another at $-25.5$ or $-27.6$ km s$^{-1}$ relative to the Sun. Such a separation is consistent with the ionization expected in H I regions where a high $n_e$ in one cloud enhances many of the neutrals. Ca II has components from all six clouds, while Ti II was found only at the two most negative velocities. The visual observations also have shown that the $CH^+$ lies entirely in the $-12.6$ km s$^{-1}$ cloud, while the radio measurement of the CO emission has demonstrated this molecule is primarily at $-14.4$ km s$^{-1}$. The lines of N II, Si III, S III, etc., which are expected to be formed in H II regions, have velocities closer to the local standard of rest than the H$\alpha$ radial velocity from the Strömgren sphere, indicating there must be additional H II in the line of sight.

The separation of ions by velocity was very useful in selecting species for the construction of the empirical curves of growth in figures 5 and 6. It is noteworthy that the curve of growth defined by C I, Na I, Mg I, and S I deviates considerably from the classical Maxwellian form, although these atoms appear to be concentrated mainly in one cloud. The empirical curves, along with some information from both the visible and ultraviolet profiles, gave the column densities in tables 7 and 8. In a number of cases, the equivalent widths or the upper limits were small enough that $N$ was nearly independent of the assumed velocity dispersion.

Calculations of the ionization equilibrium between the atoms and first ions in the average interstellar radiation field with $T = 56°$ gave an electron density $n_e = 0.7$ cm$^{-3}$ within a factor 2 for C, Mg, S, and Ca, and $n_e = 0.02$ cm$^{-3}$ for Fe. The larger $n_e$ has been adopted for the neutral cloud. Since ionized C is a more important source of electrons than ionized H, the observed ratio of C II/H requires that the density of hydrogen nuclei $n_H = 10^4$ cm$^{-3}$ in the cloud. The energy distribution of $\zeta$ Oph, after correction for interstellar absorption, is sufficiently similar to the average field that all ion ratios scale the same way if the cloud is relatively close to the star, making the derived $n_e$ and $n_H$ up to a factor 20 larger at $r = 15$ pc. Increasing the kinetic temperature to 100° would raise both densities a factor 1.5; and if a large fraction of the C II, etc., were not in the cloud they also would be higher. It has been shown by de Boer and Morton (1975) that if $n_H = 10^4$, the excited fine-structure levels of C I imply that $T = 19°$, and the observed column density of singly ionized carbon limits the thickness of the cloud to 0.05 pc, or even less if much of the hydrogen is in other clouds. These authors also have considered alternative solutions with lower densities derived entirely from the C I data, in case the $n_e$ deduced from the ionization is incorrect or the C II is not the main source of electrons. Since Na I and Ca II lines have been observed with similar radial velocities as found in $\zeta$ Oph over some 15° of sky, the absorption must occur in a very thin sheet which could be 25 pc across. However, since the reddening is greatest toward $\zeta$ Oph, the volume density may be lower and the cloud thicker toward the other stars. Herbig (1968) has argued that the star counts of Bok (1956) near $\zeta$ Oph suggest that the obscuring material and hence the principal gas cloud is at least 100 pc from the Sun. Thus the cloud must lie between 15 and 100 pc from $\zeta$ Oph, with a larger distance to be preferred unless one can accept densities of $\sim 10^5$ cm$^{-3}$.

The low temperature in the neutral cloud would prevent the excitation of the $J'' = 1$, 2, and 3 levels of $H_2$ and the formation of HD, both of which appear to have the same radial velocity as the C I. The population ratios of the $H_2$ levels imply a cloud with $56° \leq T \leq 115°$ containing at least 45 percent of the total $H_2$. Perhaps the cold cloud has a hotter, less dense outer layer. The spatial separation between C I and the excited $H_2$ is expected from their different curves of growth. The population of the excited fine-structure level of C II and the absence of O I* are consistent with $T = 19°$ and $10^4 \leq n_H \leq 2 \times 10^5$ cm$^{-3}$. Most of the C II and O I may be in the cold cloud.

Infrared radiation at 157.7 $\mu$ from the excited C II level provides the principal cooling of the H I clouds. The next important sources are lines at 28.22 $\mu$ and 17.03 $\mu$ from the rotationally excited states of $H_2$. Further analysis of the H I clouds will require models which consider the detailed processes affecting the ionization and recombination of the atoms and the formation and destruction of the $H_2$ and HD as described by Black and Dalgarno (1973*a*), Glassgold and Langer (1974), and Jura (1974*b*).

The observed size of the Strömgren sphere along with its H$\alpha$ and radio emission gave $n_e = 3$ cm$^{-3}$, or

higher if the gas is clumped. The expected Lyman continuum photons for an O9.5 V star would have produced 3 times the emission, suggesting the presence of grains which could absorb the extreme-ultraviolet photons or errors in the predicted ionizing flux.

The column densities in table 7 have provided a direct determination of the abundances of 20 elements and upper limits for five more relative to hydrogen in H I clouds. Figure 7 has shown that when the clouds are compared with the best available solar system abundances, the interstellar H I gas is depleted by factors of 3 to 4000 in most elements except S and Zn, which are close to normal, and Be and Co for which the upper limits are not yet very restrictive. The depletions generally correlate with increasing condensation temperature $T_c$, supporting Field's (1974*a*, *b*) idea that the missing material is in grains formed initially by chemical equilibrium processes in a stellar atmosphere or nebula, with later accretion of C, N, O, and Ar in dense clouds. Morton *et al.* (1974) have pointed out how the failure to detect the interstellar B II line has given an upper limit for boron which is well below the expected relation with $T_c$ unless this temperature is much higher than 700° K or the meteorites are not reliable abundance standards for this element. Table 14 has listed the evidence for the depletion of Al, Si, Ti, Cr, and Fe in the Strömgren sphere. The nitrogen abundance is close to the solar value and so may be sulfur.

## X. FUTURE WORK

This analysis of the interstellar gas in the direction of ζ Oph has indicated several areas in which additional measurements or theoretical investigations would be very useful.

From the spectroscopy laboratory, accurate wavelengths are still needed for lines of O VI, P II, Ar I, and Fe II. Kelly and Palumbo (1973) have quoted λλ1031.912, 1037.613 for the O VI resonance lines, while Morton and Smith (1973) adopted λλ1031.945, 1037.627 from Bockasten, Hallin, and Hughes (1963). If the former wavelengths were correct, it would be more reasonable to accept the unidentified feature at 1031.832 Å in the wing of HD(6,0) $R(0)$ as the short-wavelength third of a relatively broad O VI profile similar to those described by Jenkins and Meloy (1974) and York (1974). Then $W_\lambda$(O VI λ1031.9) ≈ 17 mÅ and log $N$(O VI) ≈ 13.1 since $b \geq 14$ km s$^{-1}$. The wavelengths of P II and Ar II are known to only two decimal places according to Kelly and Palumbo, and the irregularities in the Fe II points between 1090 and 1150 Å in figure 3 suggest possible errors in the wavelengths of this ion. Laboratory wavelengths also are needed for a number of Lyman and Werner lines of $H_2$. Additional analyses of ultraviolet atomic and molecular spectra should help with the identification of the lines in table 2.

Oscillator strengths are urgently needed for many transitions. The abundances or upper limits for V III, Cr II, Cr III, Fe III, Co II, Ni II, and Cu II depend entirely on rough calculations. A check on the *f*-value for Cr II λ2055.59 would be specially useful in learning whether this element is depleted more than expected from its condensation temperature. Good laboratory measurements of several of the C I lines investigated by de Boer and Morton (1975) would show if the proper curve of growth has been used for C I, Mg I, and S I, and hence if the correct electron density has been derived from the ratios with the first ions. Reliable *f*-values for S I and Cl I also would help in this test. An independent calculation for the λ1240.1 doublet of Mg II and measurements of the far-ultraviolet Fe II lines studied by de Boer *et al.* (1974) could improve confidence in the curve of growth for the ions. Checks on the *f*-values adopted by Morton and Smith (1973) for the multiplets Si II λλ1814.0, 1263.3, 1194.1, P II λλ1307.7, 1154.4, and K I λλ7676.2, 4045.2 are needed to resolve several inconsistencies in the ζ Oph analysis. No *f*-value is yet available for O I λ1039.2. Among the molecules, there are no *f*-values for three of the observed CO transitions, and the upper limits on OH, HCl, $C_2$, SiO, and $H_2O$ depend on very rough estimates. In the visible, $f$(λ4232.5) of $CH^+$ continues to be uncertain.

Some specific ultraviolet observations could help with definite questions raised in this paper. A search for the weak intersystem line of O I at 1355.6 Å could provide an O I abundance independently of the curve of growth, if the *f*-value is reliable. A tighter limit on O I* λ1304.8 would be helpful in establishing the physical conditions where O I is located. Further scans at the expected positions of the O VI lines are needed to determine the shape of the feature in the wing of the HD line and to check the existence of the ion through the detection of λ1037.6 where the continuum is weak. Another search for Cr II λ2055.6 also is desirable to confirm the surprisingly low upper limit for this ion. Other ions that may be detectable with a few consecutive scans are C IV, Si I, and Fe II*. The upper limit on Co II also could be reduced, though this ion will be difficult to detect if it is depleted as much as Fe and Ni. A search for Mg I λ1827.9 might give a valuable check on the curve of growth adopted for this atom. The limits on P III, Cl III, Ti III, V III, and Cr III could be lowered for comparison with the other elements detected in H II regions. Further scans of HD($J'' = 0$) would be useful to see if the curve of growth is similar to $H_2$, and a search for the lines of HD($J'' = 1$) could give important information on the particle density. An improved signal-to-noise ratio for the CO lines, along with profile fitting of the rotational components, would give the CO populations and the rotational temperature. Comparison with the column density obtained from the radio emission would provide a check on both analyses. A search for the $^{13}C^{16}O$ lines could give a useful second value for the ratio $^{12}C/^{13}C$ determined in a different cloud from the visible $CH^+$ lines. Additional scans of HCl λ1290.3, along with a better determination of the *f*-value, should show whether HCl/Cl I fits the high-density cloud model proposed by Dalgarno *et al.* (1974).

New ground-based observations of both K I doublets may be needed to resolve the inconsistency in

the curve of growth of this atom. A careful search for the Ti II lines in the group of clouds near $-15$ km s$^{-1}$ would show whether the depletion of this element is comparable with Ca, as expected from the condensation temperatures. A tighter upper limit for Mn I would show whether this element has the same anomalous ionization as Fe. Improved radial velocities are needed for the CH and CN lines to learn if these molecules are located in different clouds than the $CH^+$ whose formation is not understood.

More calculations of condensation temperatures are needed for appropriate temperatures, densities, and compositions. Since zinc is similar to sulfur in showing little or no depletion, it is important to have the temperature for zinc based on the same conditions as the other points in figure 1 of Morton (1974). Condensation temperatures also are needed for P, Cl, V, and Cu.

*Note added in proof.*—Improved lifetimes for P II by Livingston *et al.* (1975) give $f(\lambda 1152.81) = 0.24 \pm 0.03$ and $f(\lambda 1301.87) = 0.017 \pm 0.005$, making the $W_\lambda$'s fit the empirical curve of growth in figure 5 and eliminating the discrepancy noted in § IV*a*. In table 7 the range of $b$ is 6.0 to 5.2 km s$^{-1}$ and log $N$ lies between 13.74 and 13.92. Therefore, the depletion fraction is reduced to the range $-0.82$ to $-0.64$ in figure 7. A new $f$-value of 0.0207 for $\lambda 3859.913$ of Fe I by Bridges and Kornblith (1974) improves the fit of the two Fe I lines on the curve of growth in figure 6 and increases log $N$(Fe I) to 11.59.

The author gratefully acknowledges considerable assistance in the preparation of this paper from many individuals. Much useful information was provided by J. F. Drake, G. H. Herbig, G. Herzberg, and L. M. Hobbs. Many valuable comments were contributed by K. S. de Boer, E. B. Jenkins, M. Jura, W. A. Morton, S. R. Pottasch, J. B. Rogerson, L. Spitzer, and D. G. York. Help with the initial data reduction was given by M. P. Andrich, H. L. Dinerstein, W. L. Glennie, and J. Wrigley. The work was supported in part by the National Aeronautics and Space Administration under contract NAS5-1810 with Princeton University.

## REFERENCES


Aannestad, P. A., and Field, G. B. 1973, *Ap. J.* (*Letters*), **186**, L29.
Aldrovandi, M. V., and Pequignot, A. 1973, *Astr. and Ap.*, **25**, 137.
Allison, A. C., and Dalgarno, A. 1970, *Atomic Data*, **1**, 289.
Auer, L. H., and Mihalas, D. 1972, *Ap. J. Suppl.*, **24**, 193.
Bahcall, J. N., and Wolf, R. A. 1968, *Ap. J.*, **152**, 701.
Black, J. H., and Dalgarno, A. 1973*a*, *Ap. J.* (*Letters*), **184**, L101.
———. 1973*b*, *Ap. Letters*, **15**, 79.
Bockasten, K., Hallin, R., and Hughes, T. P. 1963, *Proc. Phys. Soc. London*, **81**, 522.
Bok, B. J. 1956, *A.J.*, **61**, 309.
Bortolot, V. J., Clauser, J. F., and Thaddeus, P. 1969, *Phys. Rev. Letters*, **22**, 307.
Bortolot, V. J., and Thaddeus, P. 1969, *Ap. J.* (*Letters*), **155**, L17.
———. 1971, *Bull. AAS*, **3**, 15.
Bridges, J. M., and Kornblith, R. L. 1974, *Ap. J.*, **192**, 793.
Conti, P. S., and Alschuler, W. R. 1971, *Ap. J.*, **170**, 325.
Curtis, L. J., and Smith, W. H. 1974, *Phys. Rev. A*, **9**, 1537.
Dabrowski, I., and Herzberg, G. 1974*a*, *Canadian J. Phys.*, **52**, 1110.
———. 1974*b*, to be published.
Dalgarno, A., Black, J. H., and Weisheit, J. C. 1973, *Ap. Letters*, **14**, 77.
Dalgarno, A., de Jong, T., Oppenheimer, M., and Black, J. H. 1974, *Ap. J.* (*Letters*), **192**, L37.
Dalgarno, A., and McCray, R. A. 1972, *Ann. Rev. Astr. and Ap.*, **10**, 375.
Dalgarno, A., and Wright, E. L. 1972, *Ap. J.* (*Letters*), **174**, L49.
de Boer, K. S. 1974, Proefschrift, University of Groningen.
de Boer, K. S., Koppenaal, K., and Pottasch, S. R. 1973, *Astr. and Ap.*, **28**, 145; **29**, 453.
de Boer, K. S., and Morton, D. C. 1975, *Astr. and Ap.*, in press.
de Boer, K. S., Morton, D. C., Pottasch, S. R., and York, D. G. 1974, *Astr. and Ap.*, **31**, 405.
de Boer, K. S., and Pottasch, S. R. 1974, *Astr. and Ap.*, **32**, 1.
Douglas, A. E. 1974, *Canadian J. Phys.*, **52**, 318.
Edlén, B., and Risberg, P. 1956, *Ark. Fys.*, **10**, 553.
Field, G. B. 1974*a*, *Ap. J.*, **187**, 435.
———. 1974*b*, *The Dusty Universe*, ed. A. G. W. Cameron and G. B. Field (Washington: Smithsonian Institution Press).
Field, G. B., and Hitchcock, J. L. 1966, *Ap. J.*, **146**, 1.
Field, G. B., Somerville, W. B., and Dressler, K. 1966, *Ann. Rev. Astr. and Ap.*, **4**, 207.
Frisch, P. 1972, *Ap. J.*, **173**, 301.
Garstang, R. H. 1961, *Proc. Cambridge Phil. Soc.*, **57**, 115.
Georgelin, Y. P., and Georgelin, Y. M. 1970, *Astr. and Ap.*, **6**, 349.
Glassgold, A. E., and Langer, W. D. 1973, *Ap. Letters*, **15**, 199.
———. 1974, *Ap. J.*, **193**, 73.
Goldstein, S. J., and MacDonald, D. D. 1969, *Ap. J.*, **157**, 1101.
Grayzeck, E. J., and Kerr, F. J. 1974, *A.J.*, **79**, 368.
Hanbury Brown, R., Davis, J., and Allen, L. R. 1974, *M.N.R.A.S.*, **167**, 121.
Herbig, G. H. 1968, *Zs. f. Ap.*, **68**, 243.
Hobbs, L. M. 1969*a*, *Ap. J.*, **157**, 135.
———. 1969*b*, *ibid.*, **158**, 461.
———. 1971, *ibid.*, **166**, 333.
———. 1972, *Ap. J.* (*Letters*), **175**, L39.
———. 1973*a*, *ibid.*, **180**, L79.
———. 1973*b*, *Ap. J.*, **181**, 79.
———. 1974, *Ap. J.* (*Letters*), **188**, L107.
Jenkins, E. B. 1973, *Ap. J.*, **181**, 761.
———. 1974, private communication.
Jenkins, E. B., Drake, J. F., Morton, D. C., Rogerson, J. B., Spitzer, L., and York, D. G. 1973, *Ap. J.* (*Letters*), **181**, L122.
Jenkins, E. B., and Meloy, D. A. 1974, *Ap. J.* (*Letters*), **193**, L121.
Johnson, H. L. 1966, *Ann. Rev. Astr. and Ap.*, **4**, 193.
Jura, M. 1974*a*, *Ap. J.* (*Letters*), **190**, L33.
———. 1974*b*, *Ap. J.*, **191**, 375.
———. 1974*c*, private communication.
Kelly, R. L., and Palumbo, L. 1973, *NRL Report*, No. 7599.
Kurucz, R. L. 1974, *SAO Special Report*, No. 360.
Kurucz, R. L., Peytremann, E., and Avrett, E. H. 1972, *Blanketed Model Atmospheres for Early-Type Stars* (Smithsonian Astrophysical Observatory).
Kusch, P., and Taub, H. 1949, *Phys. Rev.*, **75**, 1477.
Larach, D. R. 1973, Junior Paper, Princeton University.
Lassettre, E. N., and Skerbele, A. 1971, *J. Chem. Phys.*, **54**, 1597.
Lesh, J. R. 1968, *Ap. J. Suppl.*, **17**, 231.
Livingston, A. E., Kernahan, J. A., Irwin, D. J. G., and Pinnington, E. H. 1975, in preparation.
Lutz, B. L. 1974, *Ap. J.* (*Letters*), **191**, L131.

Mezger, P. G., and Höglund, B. 1967, *Ap. J.*, **147**, 490.
Mihalas, D. 1972, *NCAR Tech. Note*, STR 76.
Moore, C. E. 1970*a*, *NSRDS–NBS* 3, Section 3.
———. 1970*b*, *NSRDS–NBS* 4.
Morgan, W. W., Strömgren, B., and Johnson, H. L. 1955, *Ap. J.*, **121**, 611.
Morton, D. C. 1969, *Ap. J.*, **158**, 629.
———. 1974, *Ap. J.* (*Letters*), **193**, L35.
Morton, D. C., Drake, J. F., Jenkins, E. B., Rogerson, J. B., Spitzer, L., and York, G. 1973, *Ap. J.* (*Letters*), **181**, L103.
Morton, D. C., Jenkins, E. B., Matilsky, T. A., and York, D. G. 1972, *Ap. J.*, **177**, 219.
Morton, D. C., and Morton, W. A. 1972, *Ap. J.*, **174**, 237.
Morton, D. C., and Purcell, J. D. 1962, *Planet. and Space Sci.*, **9**, 455.
Morton, D. C., and Smith, W. H. 1973, *Ap. J. Suppl.*, **26**, 333.
Morton, D. C., Smith, A. M., and Stecher, T. P. 1974, *Ap. J.* (*Letters*), **189**, L109.
Myer, J. A., and Samson, J. A. R. 1970, *J. Chem. Phys.*, **52**, 266.
Nachman, P., and Hobbs, L. M. 1973, *Ap. J.*, **182**, 481.
O'Donnell, E. J., and Watson, W. D. 1974, *Ap. J.*, **191**, 89.
Oke, J. B., and Schild, R. E. 1970, *Ap. J.*, **161**, 1015.
Pedlar, A., and Matthews, H. E. 1973, *M.N.R.A.S.*, **165**, 381.
Penston, M. V. 1974, *M.N.R.A.S.*, **166**, 21*p*.
Pilling, M. J., Bass, A. M., and Braun, W. 1971, *J. Quant. Spectrosc. and Rad. Transf.*, **11**, 1593.
Radziemski, L. J., and Kaufman, V. 1974, *J. Opt. Soc. Am.*, **64**, 366.
Reynolds, R. J., Roseler, F. L., and Scherb, F. 1974, *Ap. J.* (*Letters*), **192**, L53.
Risberg, P. 1956, *Ark. Fys.*, **10**, 583.
Rogerson, J. B., Spitzer, L., Drake, J. F., Dressler, K., Jenkins, E. B., Morton, D. C., and York, D. G. 1973, *Ap. J.* (*Letters*), **181**, L97.
Rogerson, J. B., York, D. G., Drake, J. F., Jenkins, E. B., Morton, D. C., and Spitzer, 1973, *Ap. J.* (*Letters*), **181**, L110.
Seaton, M. J. 1951, *M.N.R.A.S.*, **111**, 390.
———. 1959, *ibid.*, **119**, 81.
Shulman, S., Bortolot, V. J., and Thaddeus, P. 1974, *Ap. J.*, **193**, 97.
Simmons, J. D., Bass, A. M., and Tilford, S. G. 1969, *Ap. J.*, **155**, 345.
Smith, A. M. 1972, *Ap. J.*, **176**, 405.
Smith, A. M., and Stecher, T. P. 1971, *Ap. J.* (*Letters*), **164**, L43.
Smith, M. W., and Wiese, W. L. 1973, *J. Phys. Chem. Ref. Data*, **2**, 85.
Smith, W. H., Liszt, H. S., and Lutz, B. L. 1973, *Ap. J.*, **183**, 69.
Solomon, P. M. 1974, *The Spitzer Symposium on Diffuse Matter in Space*, unpublished.
Spitzer, L. 1968, *Diffuse Matter in Space* (New York: Interscience).
Spitzer, L., and Cochran, W. D. 1973, *Ap. J.* (*Letters*), **186**, L23.
Spitzer, L., Cochran, W. D., and Hirshfeld, A. 1974, *Ap. J. Suppl.*, No. 266, **28**, 373.
Spitzer, L., Drake, J. F., Jenkins, E. B., Morton, D. C., Rogerson, J. B., and York, D. G. 1973, *Ap. J.* (*Letters*), **181**, L116.
Spitzer, L., and Jenkins, E. B. 1975, *Ann. Rev. Astr. and Ap.*, in press.
Spitzer, L., and Morton, W. A. 1975, in preparation.
Spitzer, L., and Zweibel, E. G. 1974, *Ap. J.* (*Letters*), **191**, L127.
Thuan, T. X. 1975, *Ap. J.*, in press.
Tilford, S. G., Ginter, M. L., and Vanderslice, J. T. 1970, *J. Mol. Spectrosc.*, **33**, 505.
Torres-Peimbert, S., Lazcano-Araujo, A., and Peimbert, M. 1974, *Ap. J.*, **191**, 401.
Traub, W. A., and Carleton, N. P. 1973, *Ap. J.* (*Letters*), **184**, L11.
Uesugi, A., and Fukuda, I. 1970, *Contr. Inst. Ap. and Kwasan Obs., Univ. Kyoto*, No. 189.
Vanden Bout, D. A. 1972, *Ap. J.* (*Letters*), **176**, L127.
Wallerstein, G., and Goldsmith, D. 1974, *Ap. J.*, **187**, 237.
Watson, W. D. 1974, *Ap. J.*, **189**, 221.
White, R. E. 1973, *Ap. J.*, **183**, 81.
Wiese, W. L., Smith, M. W., and Glennon, B. M. 1966, *NSRDS–NBS* 4.
Wilkinson, P. G. 1968, *Canadian J. Phys.*, **46**, 1228.
Withbroe, G. D. 1971, *The Menzel Symposium* (NBS Special Pub. 353), ed. K. B. Gebbie (Washington: Government Printing Office).
Witt, A. N., and Johnson, M. W. 1973, *Ap. J.*, **181**, 363.
York, D. G. 1974, *Ap. J.* (*Letters*), **193**, L127.
York, D. G., Drake, J. F., Jenkins, E. B., Morton, D. C., Rogerson, J. B., and Spitzer, L. 1973, *Ap. J.* (*Letters*), **182**, L1.
Yoshimine, M., Green, S., and Thaddeus, P. 1973, *Ap. J.*, **183**, 899.

DONALD C. MORTON: Princeton University Observatory, Princeton, NJ 08540